FINITE ELEMENT MODELLING OF REINFORCED CONCRETE SLAB

A Thesis Report submitted in the partial fulfillment of

requirement for the award of the degree of

MASTER OF ENGINEERING

IN

STRUCTURES

Submitted By

Priya Bansal

Roll No. 801122012

Under the Supervision of

Dr. Naveen Kwatra

Head and Associate Professor,
Department of Civil Engineering
Thapar University, Patiala

DEPARTMENT OF CIVIL ENGINEERING

THAPAR UNIVERSITY,

PATIALA- 147004, (INDIA).

JULY-2013

DECLARATION

I hereby declare that the work which is presented in this thesis report entitled "**Finite Element Modelling of Reinforced Concrete Slab**", in partial fulfillment of the requirement for the award of degree of **MASTER OF ENGINEERING (STRUCTURAL ENGINEERING)** in the **CIVIL ENGINEERING DEPARTMENT, THAPAR UNIVERSITY, PATIALA**, is a n authentic record of the initial work carried out by her under the supervision of **Dr. Naveen Kwatra, Head and Associate Professor,** DEPARTMENT OF CIVIL ENGINEERING, THAPAR UNIVERSITY, PATIALA.

The matter embodied in this report has not been submitted in part or full to any other university or institute for the award of any degree.

Priya

Date: 15-07-2013 (PRIYA BANSAL)

This is to certify that the above declaration made by the student concerned is correct to the best of my knowledge and belief.

19/7/13

(Dr.Naveen Kwatra)
Head and Associate Professor,
Deptt. of Civil Engineering,
Thapar University, Patiala

(Dr. S.K. Mohapatra)
Dean Academic Affairs
Thapar University,
Patiala

ACKNOWLEDGEMENT

A dissertation cannot be completed without the help of many peoples who contribute directly or indirectly through there constructive criticism in the evolution and preparation of this work. It would not be fair on my part, if I don't say a word of thanks to all those whose sincere advice made this period a real educative, enlightening, pleasurable and memorable one.

I would like to express my deepest appreciation to my thesis supervisor, Head and Associate Professor **Dr. Naveen Kwatra** for their gracious efforts and keen pursuits, which has remained as a valuable asset for the successful instrument of my Thesis Report. His dynamism and diligent enthusiasm has been highly instrumental in keeping my spirit high. His flawless and forthright suggestions blended with an innate intelligent application have crowned my task a success.

I would also like to express my gratitude to my family, for their unconditional support and prayers at all times and constant encouragement during the entire course of my thesis work.

I am also like to offer my sincere thanks to all faculty, teaching and non-teaching of Civil Engineering (CED) TU, Patiala for their assistance. Thank you.

PRIYA BANSAL

M.E CIVIL STRUCTURES

ROLL NO 801122012

ABSTRACT

Strengthening of reinforced concrete (RC) structures is frequently required due to inadequate maintenance, excessive loading, change in use or in code of practice and exposure to adverse environmental conditions. Several strengthening techniques have been developed in the past and used with some popularity including steel plate bonding, external pre-stressing, section enlargement whereas now-a-days a new strengthening systems, such as fibre reinforced polymers (FRPs), that have the potential for extending the service lives of RC structures and reducing maintenance costs is used. Structural rehabilitation needs, strengthening and retrofitting of concrete structural parts has now-a-days become the major growth research area for the researchers. External wrapping with fiber-reinforced polymer (FRP) is a promising solution for retrofitting due to various advantages such as high strength-weight ratio, corrosion resistance, ease of application, low labour costs, and no significant increase in member size over other strengthening techniques. In particular, the flexural strength of a slab can be significantly increased by application of FRP sheets adhesively bonded to the tension face of the slab.

It was difficult to model the complex behaviour of reinforced concrete structures analytically in its non-linear zone. This has led engineers in the past to rely heavily on empirical formulas which were derived from numerous experiments for the design of reinforced concrete structures.

Nowadays, for structural design and assessment of reinforced concrete members, the non-linear finite element (FE) analysis has become an important analytical tool. But a very limited work is done on the use of FEM to analyze retrofitted RC slabs. The finite element method accounts for non-linear response. The finite element method allows complex analysis of non-linear response of RC structures to be carried out in a simpler way. The finite element method (FEM) also helps in investigating the behaviour of the structure under different loading conditions, the load deflection behaviour of the structure and the cracks pattern.

The present study deals with the finite element modelling of control RC slab, retrofitted slab and stressed retrofitted slabs with the help of ATENA. ATENA is software that is based on FE method in which modelling of RC structures is done. In this thesis, a control slab was modelled and the results were analyzed and then retrofitted and stressed retrofitted slabs were modelled and analyzed. The results of the control and retrofitted slabs were compared with the experimental results and the results of the stressed retrofitted slabs were compared with that of

the control slab. Four simply supported full scale slabs were modelled and area load was applied on the top surface of the slab, surface of the slab, out of which one slab was taken as control slab, one slab as retrofitted slab and rest two slabs were stressed at 75% and 90% and they are then retrofitted by using the GFRP sheet.

In the first phase, the control slab was modelled and analyzed. Then the retrofitted slab was modelled and analyzed and then the ultimate load carrying capacity, load-deflection behaviour, crack propagation and crack pattern were noted at different steps. After that the retrofitted slabs were modelled and were stressed to their respective loads, then retrofitted with GFRP layer and results of stressed retrofitted slabs were analyzed and compared with the control slab.

In the second phase, the results of all the RC slabs were compared. The results of both control and retrofitted slabs were compared with the experimental results and the results of stressed retrofitted slabs were compared with the results of control slab. From the results it was seen that ultimate load carrying capacity of the stressed retrofitted slabs was higher than the control slab. A close agreement of analytical results was seen with the experimental results.

TABLE OF CONTENTS

LIST OF TABLES

LIST OF FIGURES

CHAPTER 1 INTRODUCTION

1.1 GENERAL

Reinforced Concrete is one of the most versatile construction materials used in civil engineering. Slabs are plane structural members whose thickness is quite small as compared to its span and width. In reinforced concrete construction, slabs are most frequently used as structural elements forming roof covering, floors and bridges. Slabs may be supported by reinforced concrete beams or directly by columns. It usually carries uniformly distributed gravity load acting normal to its surface and transfers same to the supports by flexure, shear and torsion. Therefore because of its complex behavior it is difficult to decide whether the slab is a structural component, structural element, or structural system in itself.

The damage in the RC structures occurs due to various reasons like cracking of concrete, concrete spalling or due to large deflections etc. The deterioration in the structures are due to various factors such as change in use, change in design configuration, corrosion of steel, increasing load on the structure, inferior building material and environmental effects. Repair and rehabilitation has become an important aspect for the reinforced cement concrete structures.

1.2 NECESSITY OF STRENGTHENING REINFORCED CONCRETE SLABS

The situations in which the reinforced concrete slabs require the intervention for repairs or strengthening are the following [1]:

a) Repairing damaged/deteriorated concrete slabs to restore their strength and stiffness.

b) Corrosion of the reinforcement.

c) Limiting crack width under increased (design/service) loads or sustained loads.

d) Retrofitting concrete members to enhance the flexural strength and strain to failure of concrete elements requested by increased loading conditions such as earthquakes or traffic loads.

e) Rectifying design and construction errors such as undersized reinforcement.

f) Enhancing the service life of the RC slabs.

g) Shear strengthening around columns for increasing the perimeter of the critical section for punching shear.

h) Changes in the structural system such as cut-outs in the existing RC slabs.

i) Changes of the design parameters.

j) Optimization of structure regarding the reduction of deformations and of the stresses in the reinforcing bars.

1.3 RETROFITTING USING FIBER REINFORCED POLYMERS (FRP)

Besides the use of different conventional methods used to repair and retrofit the concrete structures like adding of shear wall, jacketing etc., strengthening with the use of fiber reinforced polymer (FRP) is one of the techniques which has wide range of scope and is extensively used these days. Continuing advances in the manufacturing techniques and performance of fibre-reinforced polymer (FRP) materials have allowed FRPs to move from playing a secondary role in civil infrastructure to one that is a genuinely feasible construction alternative. This is a new technique having tremendous potential. FRP is a composite material made by combining two or more materials to give a new combination of properties. FRP composite is a two-phased material and is composed of fiber and polymer matrix, which are bonded at interface as shown in Figure 1.1. The fibers are usually glass, carbon, aramid while the polymer is usually epoxy, vinyl ester. Fibers provide FRP composite with strength and stiffness, while the matrix gives rigidity and environmental protection. Fibers can be used in its two forms: fiber wraps or sheets and fiber laminates.

The technology for external retrofitting was developed primarily in Japan (sheet wrapping) and Europe (laminate bonding). Today there are more than 1000 concrete slab/steel girder bridges in Japan that have been strengthened with sheet bonding to the slabs. Reduced material cost, coupled with labor savings inherent with its low weight and comparably simpler installation, relatively unlimited material length availability, and immunity to corrosion, make FRP materials an attractive solution for post strengthening, repair, seismic retrofit, and infrastructure security.

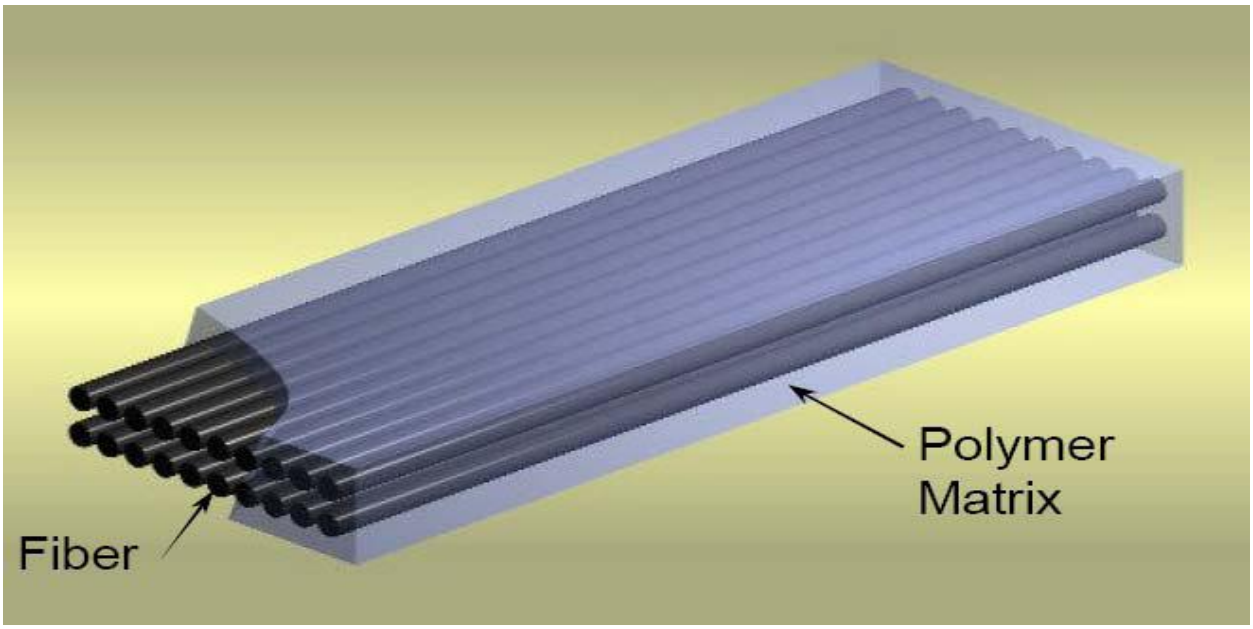

Figure 1.1 Formation of FRP composite

Retrofitting of concrete beams and columns is quite common these days but nowadays retrofitting of slabs is also coming into picture. The FRP laminates are bonded to the bottom surface of the slab to increase the strength and stiffness of the slab. The delamination of the FRP layer is seen in the slab. This delamination of the FRP layer can be controlled or reduced by anchoring the bonded layer by fiber anchors which in turn also increases the load carrying capacity of the slab. The bond between the concrete substrate and the FRP laminate should be proper for lesser debonding. The selection of the most appropriate method to use will depend on several factors, such as the amount of strengthening required, the location where strengthening is required, architectural requirements, simplicity and speed of application, and total cost. The fiber wrapping on the slab is done as shown in Figure 1.2.

Fiber reinforced polymers (FRP) have great potential for use in civil infrastructure applications. They offer a number of advantages over conventional materials such as:

- Superior strength to weight ratio;
- Superior stiffness to weight ratio;
- Superior electromagnetic properties;
- Excellent fatigue damage tolerance;

Figure 1.2 Fiber wrapping of the slab [15]

Chothani. D.G. studied experimentally the effect of GFRP sheet on the ultimate strength of the slab. Wrapping the slab with the help of FRP layer increases the flexural strength of the slab and increases the life period of the slab. From the three slabs which were tested, one slab was taken as control slab(without strengthening), second was bonded with the layer of GFRP at the bottom surface of the slab using epoxy resin and the third slab, the GFRP layer was bonded as well as anchored with the slab to further increase the flexural strength of the slab. The slab was tested under one-way condition and a uniformly distributed load was applied on the slab through hyraulic jack. Whereas in the present thesis work, analytical work has been carried out to observe the load carrying capacity, load deflection curve and the crack patterns at different load steps using non-linear analysis method of the control slab, retrofitted slab and the stressed retrofitted slabs. In the analytical work, load is applied in the form of area load on the surface of the slab. The analytical results obtained from finite element modelling are compared with the experimental results. The cracks appeared on the partially failed slabs need to be retrofitted to gain some strength. It is required to study the stressed retrofitted slabs at different stress levels. So in this study, the stressed retrofitted slabs are also analyzed.

The finite element method allows complex analysis of the nonlinear response of RC structures. FEM helps in investigating the behaviour of the structure, before and after the loading conditions, its load- deflection behaviour and the cracks pattern. The analytical results of finite element models have to be evaluated by comparing them with experiments of full-scale models of structure. The development of reliable analytical models can, however, reduce the number of required test specimens for the solution of a given problem whereas conducting those tests experimentally are time-consuming and costly and they often do not simulate exactly the loading and support conditions of the actual structure.

1.4 OBJECTIVES

The main objective of the present study is to investigate the non linear response up to failure of RC slabs and retrofitted RC slabs using FE modelling under incremental loading and is intended to investigate the relative importance of several factors in non linear finite element analysis of RC slabs. These include the variation in the load-displacement graph, the crack patterns, propagation of cracks, the crack width and the effect of non-linear behavior of concrete and steel on the response of control slab and the deformed slab.

The following are the main objectives of the present study:

1. To model the reinforced cement concrete slab called as control slab, the retrofitted slab and the stressed retrofitted reinforced cement concrete slabs at 75%and 90% using FEM.
2. To determine analytically the load deflection curve of control slab, retrofitted slab and the retrofitted slabs stressed at 75% and 90%.
3. Compared the results of control slab and the stressed retrofitted slab and also compared the analytical results with the experimental results.

1.5 SCOPE OF THE WORK

In the first phase of the present study, Finite Element Modelling of the control RC slab under the incremental loads has been analyzed using ATENA software and the results so obtained have been compared with available experimental results from the work done by Dipak G. Chothani,

Narendra K. Arora and Sweta P. Dave (2012). The size of slab is 1500mm x 900mm x 50mm with uniformly distributed load. The slab is simply supported at 1300mm centre to centre distance. The materials which are used in the modeling are M 25 concrete and Fe 722 reinforced bars of 4mm were used as reinforcement.

The control slab is analyzed using ATENA software up to the failure and then gets the load deformation curves and the cracking behaviour is monitored. The control slab has been analyzed and results have been compared with the experimental results.

In the second phase of the present study, FE modelling of the retrofitted RC slab is analyzed using ATENA software and the load- displacement curve, maximum load carrying capacity and the cracking behaviour are also obtained analytically.

In the third phase of the present study, FE modelling of the stressed retrofitted RC slabs at 75% and 90% is done and is then analyzed. The retrofitting of the slabs is done by using GFRP. The analytical results of the slab are compared with the experimental results. Comparisons are made by the load deflection curves and values. Deflection and cracking behaviour of the RC slabs are also studied.

The following parameters are proposed to be measured:

i) Nonlinear load- deflection behavior.

ii) Study of crack pattern at different load steps.

iii) Level/type of damage and location of damage.

1.6 IMPORTANCE OF FINITE ELEMENT MODELLING

To model the complex behavior of reinforced concrete analytically in its non-linear zone is difficult. It has led engineers in the past to rely heavily on empirical formulas which were derived from numerous experiments for the design of reinforced concrete structures. The Finite Element method makes it possible to take into account non-linear response. The FE model is an analytical tool which is able to model RCC structure and is able to calculate the non-linear behaviour of the structural members is Finite Element method. Each element in a finite element model will have a fixed number of nodes that define the element boundaries to which loads and boundary conditions can be applied. The finer the mesh, the closer we can approximate the geometry of the structure, the load application, as well as the stress and strain gradients.

However, there is a tradeoff: the finer the mesh, the more computational power is needed to solve the complex problem. The strategy of optimizing the mesh size can greatly reduce an analyst's time without compromising on the quality of analysis results. For structural design and assessment of reinforced concrete members, the non-linear finite element (FE) analysis has become an important tool. The method can be used to study the behaviour of reinforced and pre-stressed concrete structures including both force and stress redistribution.

With the advent of digital computers and powerful methods of analysis, such as the finite element method many efforts to develop analytical solutions which would obviate the need for experiments have been undertaken by investigators. The finite element method has thus become a powerful computational tool, which allows complex analyses of the nonlinear response of RC structures to be carried out in a routine fashion [2].

FEM is useful for obtaining the load deflection behaviour and its crack patterns in various loading conditions. The finite element method has a number of advantage, they include the ability to:

a. Model irregularly shaped bodies and composed of several different materials.
b. Handle general load condition and unlimited numbers and kind of boundary conditions.
c. Include Dynamic effects.
d. Handle nonlinear behavior existing with large deformation and non linear material

1.7 ORGANIZATION OF THE THESIS

The thesis is divided into five chapters and is organized as per detail given below:

Chapter 1: Introduces to the topic of discussion in brief.

Chapter 2: Discusses the literature review i.e. the work done by various researchers in the field of FE modelling of RCC slabs and retrofitted structural members.

Chapter 3: First part deals with the FEM modelling, theory related to the ATENA, material modelling and it also deals with the description of the material behaviour of concrete, reinforced steel bars. Second part comprises of details of the structure modelled in ATENA and

the analytical programming procedure steps involved in modelling of the RCC slabs.

Chapter 4: The results from the analysis, comparison between the analytical and the experimental results, results comparison between the control slab and stressed retrofitted slabs and the cracking behaviour of the slabs, all are discussed in this chapter.

Chapter 5: Finally, salient conclusions and recommendations of the present study are given in this chapter followed by the references.

CHAPTER 2 LITERATURE REVIEW

2.1 GENERAL

In order to contextualize the current work, related works from literature is discussed. A detailed review related to the retrofitted reinforced cement concrete slabs would be too immense to address in this chapter. However, there are many good references that can be used as a starting point for research. In this chapter the research work concerning to the various applications and methods used for testing of the slabs are discussed and will focus on recent contributions related to the retrofitting techniques of the RCC slabs, materials used for retrofit.This literature review gives a comprehensive review of the work carried out by various researches in the field of RCC slabs and retrofitting of slabs.

2.2 FINITE ELEMENT MODELLING AND THE RETROFITTING OF RC SLABS

Chothani D.G. et al., (2012) studied the effect of GFRP sheet on ultimate strength of slab. The structural response of slab was improved due to FRP laminate bonded on the slab. In the experimental work, three identical reinforced concrete slabs (1500x900x50mm) were constructed. All the slabs were reinforced with 4mm diameter steel rods. The steel rods were placed at 150mm centre to centre in both the directions and were tied by the binding wires with 10mm cover provided to the rods. Out of the three slabs, one slab was taken as control slab i.e. slab without any FRP laminate, second slab was strengthened with a layer of GFRP which was bonded at the bottom with the help of epoxy resin and the third slab was strengthened with a GFRP sheet which was bonded at the bottom as well as anchored to the slab. The grade of concrete used was M25 and the proof stress of the steel rod was 722 MPa and the ultimate stress was 807MPa. All the three slabs were simply supported at 1300mm centre to centre distance and were tested under one-way condition. A uniformly distributed load was applied on the slab through a hydraulic jack and the deflection of the slab was noted at three locations i.e. at one-fourth, at centre and at three-fourth of the span. In the third slab, aluminium spacer tube was attached to the base through nuts and bolts to facilitate anchorage. The GFRP sheets used in the experimental work were bi-directional and thickness of the sheet used was 1mm. the ultimate

tensile strength of the GFRP sheet in one direction was 31363.6 MPa. The load-deflection response, ultimate load- carrying capacity was noted during the experiment.

Slabs containing GFRP sheets showed regain in stiffness whereas the slab having no GFRP laminate showed negligible improvement in stiffness. The ultimate load carrying capacity of the slab with bonded GFRP sheet was increased by 27.12% whereas for the slab which is bonded as well as anchored with GFRP sheet showed 79.97% increase in ultimate load carrying capacity as compared to the control slab. GFRP sheet showed no participation during initial linear stage as first crack load was almost same for all the slabs. De-lamination of GFRP sheet was noticed at few locations from the slab. The overall performance of bonded and anchored GFRP slab and bonded GFRP slab was better than the slab without any GFRP sheet [3].

Kenneth W.N. et al., (2011) presented the non-linear finite element method of reinforced concrete members externally strengthened with FRP which includes the flexure and shear strengthening of beams and FRP strengthening of two-way slabs. For strengthening of slabs both externally bonded and mechanically fastened FRP techniques were used. A non-linear appropriate model was incorporated to represent the interfacial behaviour between bonded/fastened FRP laminates and the concrete substrate. The ultimate load carrying capacity, load-deflection relationship and the failure modes are analyzed analytically and then were compared with the experimental results. The bond stress-slip model was incorporated to simulate the FRP/concrete interfacial behaviour accurately by using interface elements. The model used in this study for FRP/concrete behaviour was provided in the ADINA software. The average numerical to experimental load carrying capacity for FRP flexural strengthened beam was 100.3% and the average value for FRP shear strengthened beam was102% showing an excellent agreement between both experimental and analytical results. In case of FRP strengthened slab with externally bonded FRP, the average load carrying capacity ratio was 97% and for mechanically fastened two-way slab, reasonable accuracy was obtained between experimental and the analytical results. The members either fail by FRP debonding from the plate ends or may fail due to rupture of concrete. The load-deflection curves determined analytically also showed good agreement with the experimental load-deflection curves. In order to accurately predict the behaviour of externally FRP strengthened members, FRP/concrete interface should be appropriately modelled. [4]

Kim Y.J. et al., (2008) studied the effectiveness of two-way slabs strengthened with prestressed or nonprestressed carbon fiber reinforced polymer (CFRP) sheets. A nonlinear 3-D finite-element analysis used ANSYS. The results obtained from the ANSYS finite element analysis are compared with the experimental data for four large-scale two-way slabs (3000x3000x90)mm in which one slab was taken as unstrengthened slab, one slab was strengthened with nonprestressed CFRP sheets and two slabs with prestressed CFRP sheets. Monotonic load was applied at the centre of the span. The comparisons are made for the flexural behaviour including the load-deflection response, strain distribution, crack propagation. An increase in the flexural load-carrying capacities of up to 25% and 72% experimentally and 32% and 80% in the finite element analysis was achieved for the slab strengthened with nonprestressed and prestressed CFRP sheets respectively as compared to the unstrengthened control slab. Failure of the control slab was very ductile and the strengthened slabs failed because of the delamination or partial rupture of the CFRP sheets. In the tested slabs, orthogonal and diagonal crack propagations were observed. Large crack openings and high local strains were also observed in the steel and the CFRP sheets under the loading area [5].

Maaddawy T.E. et al., (2008) examined the reinforced concrete slabs which were mechanically anchored with unbonded FRP system. Both ultimate load carrying capacity and mid-span deflection are studied. In the experimental work, six reinforced concrete slabs with size 1800mmx500mmx100mm were constructed. All the slabs were reinforced with 0.8% steel reinforcement ratio while the strengthened slabs had 0.12% external CFRP reinforcement ratio. Out of these six slabs, one slab was taken as control slab i.e. without any strengthening system and rest five were strengthened with FRP system. From these five slabs, two were externally bonded (EB) with FRP (1 with end anchorage and other without end anchorage) and three slabs were mechanically anchored (MA) with unbonded FRP with different anchor locations. Presence of end anchorage in EB-FRP prevents delamination of CFRP strips which in turn increases the ultimate load of slab up to 62% than that of control slab and also decreases the mid-span deflection.MA-UFRP showed an increment of 43% in the slab flexural strength. The strength of the slabs strengthened with MA-UFRP system was 18% lower than that of the slab strengthened with EB-FRP system with end anchorage but only 10% lower than that of the slab strengthened

with EB-FRP system without end-anchorage. The mid-span deflection at ultimate load of the slabs strengthened with MA-UFRP system was on average 56% higher than that of the slab strengthened with EB-FRP without end-anchorage, 5% higher than that of the slab strengthened with EB-FRP with end-anchorage, and only 15% lower than that of the control. The slab which was bonded but not anchored failed by FRP delamination and rest of the slabs failed by concrete crushing [6].

Elsayed W. et al., (2007) presented the finite element analysis that was carried to simulate the non-linear load-deflection behaviour and failure mechanisms for reinforced concrete two-way slabs strengthened with externally bonded fibre reinforced polymers. The numerical analysis is carried out using the finite-element software package ADINA. The FRP/concrete interfaces were modeled using appropriate elements connecting the FRPs to the concrete substrate. These interface elements were characterized by specific bond-slip relationships that account for debonding failures and through this ultimate capacities and other failure modes were also to be predicted. Comparisons were made between the experimental and numerical results in terms of the ultimate load carrying capacities and load-deflection relationships. The numerical analyses were able to properly simulate slabs strengthened in either shear or in flexure, with various FRP strengthening configurations. Two bond-slip laws (bilinear and nonlinear) were employed in the analyses. Both the models led to virtually identical predictions. Whereas analyses based on a perfect bond between the FRP and concrete led to over predictions of the ultimate capacities and stress levels in the bonded FRPs. So no debonding was seen in the perfect bond analysis. This analysis shows many parameters that affect the performance of strengthening schemes. It was seen that increasing the width of FRP laminate led to decrease in the interfacial shear stresses and slips. The regions where the FRP laminates overlap, reductions in the interfacial stresses and slips were observed. A good agreement was seen between the analytical and experimental results. [7]

Limam O. et al., (2005) analyzed the strengthening of reinforced concrete two-way slabs with CFRP (carbon fibre reinforced plastic) strips bonded to the tensile face. Two similar RC two-way slabs with cross-section 70 mm×1150 mm×1650 mm were tested. The internal steel reinforcement consists of 6 mm diameter bars. The RC slabs were supported on four sides and

were subjected to load at the centre and the deflection is also observed at centre of the slabs. A two-dimensional finite element for composite orthotropic plate was used to describe elastic behaviour of RC two-way slabs. The results obtained from 2-D finite element analysis are compared with the experimental data for two slabs. The comparisons are made for load-deflection curves at mid-span as the load is applied at the centre. The results from finite element analysis were calculated at the same location as that of the experimental test of the slabs. The accuracy of the finite element models is assessed by comparison with the experimental results, which were to be in a good agreement. The load-deflection curves from the finite element analysis as well as from the experimental are in the linear range up to 40 kN and the complete debonding of CFRP strips with some concrete which still bonded on it was observed when the load rises up to 87 kN for slab A and 79 kN for slab B. The analytical results showed lesser deflection as compared to the experimental results. [8]

Limam O. et al., (2003) conducted an experimental investigation on RC two-way slabs strengthened with CFRP strips which are bonded on the tension face of the slab and compared them with the analytical results. In this study, debonding of external FRP strip from slab was presented. In the experimental program, two slabs were constructed and tested. The cross-section of the slabs was 1700x1300x70mm and these slabs were provided with 6mm diameter internal steel reinforcement bars. In the analytical procedure, a simplified laminated plate model was used to describe the behaviour of 3 layered plate. Two slabs were considered and tested in which one slab was taken as control slab (without strengthening) and the other slab was strengthened with CFRP strips bonded to the tension face. The ultimate loading capacity of the control (non-strengthened) slab is about 48 kN whereas the ultimate load capacity of the strengthened slab is about 120 kN. The non-strengthened slab presents more ductility than the strengthened one and presents a failure mode with diagonal yield lines, however, complete debonding of CFRP strips with some concrete which still bonded in it was seen in the FRP strengthened slab. Good agreement was made between experimental and analytical results as ultimate load carrying capacity was almost similar i.e. 120 kN experimentally and 123kN analytically for the strengthened slab. The use of CFRP strips were effective in strengthening of slabs as the load carrying capacity of control slab was much less than the strengthened slab and the deflection of control slab was much higher than the strengthened slab [9].

Mosallam A.S. et al., (2003) presented the ultimate response of unreinforced and reinforced concrete slabs repaired and retrofitted with fiber reinforced polymer (FRP) composite strips. Both carbon/epoxy and E-glass/epoxy composite systems were used in this study. The experimental results were compared with the analytical results. In the experimental study, ten slabs of size 2670x2670x76mm were tested and repaired/retrofitted with both carbon and E-glass fibres. Both carbon and glass fibers are effective in upgrading the structural capacity of both two-way unreinforced and reinforced concrete slabs. The finite element method was used to predict the behaviour of repaired slabs. For repaired unreinforced concrete slabs, use of composite systems not only restores the original capacity of damaged slab but also increases the strength of repaired slab to more than 540% of original capacity of control slab and no major failure occurred except the debonding of E-glass/epoxy in these slabs. For retrofitted slabs, use of FRP upgrades the structural capacity up to 500% for unreinforced specimen and 200% for steel reinforced specimen. In unreinforced slabs retrofitted with E-glass/epoxy, a localized compression failure of concrete was common mode of failure with some localized debonding near the ultimate load. In all cases, the failure was preceded by relatively large deformations which provided visual warning before ultimate failure. A good agreement was seen between the analytical and experimental results [10].

Lam L. et al., (2001) examined the strengthening of RC cantilever slabs using bonded glass fiber reinforced plastic (GFRP) strips. Cantilever slabs with steel reinforcement of different amounts and different positions were considered and the effect of preloading on the strength of slabs was studied. In this study, four cantilever slabs were prepared and the size of the slabs was 700mm long, 500mm wide and 100mm thick. First two slabs had same steel reinforcement ratio and position but the first slab was loaded before strengthening to consider the effect of pre-cracking. In the third slab, the steel bars were located far away from the tension face whereas the fourth slab had higher steel reinforcement ratio as compared to all other three slabs. All the slabs were strengthened with two GFRP strips and all the slabs were fixed on stiff support. The load was applied horizontally using hydraulic jack. At the initial stages, behaviour was almost linear and after the cracks started appearing the behaviour changed the linear path. The GFRP strips were anchored to the supporting wall using epoxy-mortar–filled horizontal slots and anchored to

the slab using fiber anchors to prevent or reduce debonding. Debonding between the slab and the GFRP strips is less likely to occur as they are arrested by the fiber anchors due to proper anchorage of the FRP strips to the cantilever slab but in first two slabs de-lamination occurred at 91% for the first slab and 85% for the second slab of the ultimate load but delamination was controlled by the fibre anchors. All the strengthened slabs failed by tensile rupture of FRP because of fiber anchors and some of the slabs showed partial debonding before the FRP rupture took place. The effect of preloading due to self-weight and service loads is generally insignificant if the slab fails by FRP rupture whereas the effect becomes more significant and detrimental if the slab fails by concrete crushing. [11]

Teng J.G. et al., (2001) presented an experimental study on reinforced concrete (RC) cantilever slabs bonded with glass fibre-reinforced polymer (GFRP) strips. Ten different tests in three series were conducted on RC cantilever slabs with different amounts of internal steel reinforcement and different external FRP reinforcement. The nominal cross-section of the slabs were taken as 700x500x100mm and all the slabs were supported in a stiff support. Three different steel reinforcement ratios used were 0.503%, 0.283% and 0.785%. In all the series first specimen was taken as control slab. In first series, second and third slabs were bonded with two 1-layer FRP strips of different widths i.e. 40mm and 80mm respectively and external FRP reinforcement ratio was 0.203% and 0.406%. One extra specimen was tested in series 1 that was bonded with two double layer FRP strip with 80mm width and FRP reinforcement ratio of 0.813%. In rest both the series 40mm and 80mm widths were used respectively for 2^{nd} and 3^{rd} specimen. In all the FRP-strengthened slabs, debonding of FRP strips started near the fixed end and propagated towards the free end of the slab. Complete debonding of GFRP strip or FRP tensile rupture were the failure modes that occurred in the slabs. The internal steel reinforcement ratio is not a major factor to account for the possibility and amount of debonding rather it depends on the thickness and width of the bonded FRP strips. The maximum load was taken by the slabs which had maximum thickness and width as in series-A maximum load of 23.96kN was taken by the fourth specimen, in series-B maximum load of 19.84kN was taken by second specimen and in series-C maximum load was 24.05kN which was taken by third specimen. Debonding in these slabs does not have a serious detrimental effect on the ultimate strength,

particularly when the FRP reinforcement ratio was low; instead debonding led to a more ductile behaviour. [12]

2.3 GAPS IN RESEARCH AREA

Many researchers have done work both experimentally and analytically in the area of strengthening and retrofitting the structural members with composite materials. The concept of retrofitting the structural members is rapidly increasing nowadays because of the advantage of early identification of damage and as they also provides warning for unsafe condition. Some researchers have also investigated on the area of the failure mode of the FRP strengthened structural members and some had worked on the strengthening of the structural members with different FRP materials.

In this thesis, research is concerned with the finite element modelling of the retrofitted the RC slab using the GFRP. The use of GFRP sheets for retrofitting and the strengthening of the reinforced concrete structures have been studied extensively in previous studies. However, many researches performed work both experimentally and analytically on the strengthening of the beams/columns as discussed earlier but limited work has been done on field of RCC slabs and also on the stressed retrofitted slab. That's why, with the help of ATENA, it is possible to model the stressed retrofitted slab and then analyze it. ATENA also helps in the finite element modelling of RC slab and meshing inside the surface of the slab. It gives the load deflection curve and it also gives the values of stress-strain, crack width of the slab and the material of the slab at every step which helps in modelling the deformed slab.

2.4 CLOSURE

The literature review has suggested that use of a finite element modelling of the RCC control slab and the retrofitted reinforced cement concrete slab is indeed feasible. So it has been decided to use ATENA for the FE modelling. With the help of this software study of RCC slab has been done. ATENA also helps in FE modelling and meshing inside the surface of element. It gives the load deflection curve and gives the values of stresses and strains, crack width of the elements of the slab at every step.

Chapter 3 FE MODELLING OF RC SLAB

3.1 GENERAL

From last two three decades, numerical simulation of reinforced concrete structures and structural elements has become a major area of research. Choosing suitable elements, formulating proper material models and selecting proper solution method are required for a successful numerical simulation. In this chapter, description of the structure is given that is to FE modeled and analyzed to obtain load deformation analytically.

This chapter discusses the theory related to ATENA and information about finite elements currently implemented in ATENA. In this chapter, all the necessary steps to create these models are explained in detail and the steps taken to generate the analytical load-deformation response of the model are discussed. In the experimental work done by Chothani D.G., the load has been applied in the form of point load which is further distributed on the whole surface of the slab. Therefore, the area load applied on the surface of the slab analytically is converted into equivalent point load.

3.2 INTRODUCTION TO FE MODELLING

3.2.1 Finite Element Method

FEM is a numerical technique to find approximate solutions for boundary value problems, for partial differential equations and also for integral equations. These differential equations are solved by either eliminating the differential equations completely or by rendering these differential equations into ordinary differential equations which are then numerically integrated using standard techniques. Finite Element Method is a good choice for solving partial differential equations over complex domains.

How does FE Method works:

1. Discretize the Continuum.
2. Select Interpolation Functions.
3. Find the material properties.
4. Assemble the material Properties to Obtain the System Equations.

5. Impose the Boundary Conditions.
6. Solve the System Equations.
7. Make Additional Computations if desired.

3.2.2 Applications of Finite Element Method

1. FEM allows detailed visualization of where structures bend or twist, and indicates the distribution of stresses and displacements.
2. FEM can readily handle very complex geometry.
3. FEM can also handle complex loading.
4. FEM allows entire designs to be constructed, refined, and optimized before the design is manufactured.
5. FEM provides stiffness and strength visualizations.
6. FEM also provides a wide range of simulation options for controlling the complexity of both modelling and analysis of a system.

3.3 FINITE ELEMENT MODELLING

The finite element method (FEM) is the dominant discretization technique in structural mechanics. The concept of FEM modelling is the division of mathematical model into non-overlapping components of simple geometry. The response of each element is expressed in terms of a finite number of degrees of freedom characterized as the value of an unknown function.

The finite element method is well suited for superimposition of material models for the constituent parts of a composite material. Advanced constitutive models implemented in the finite element system ATENA serve as rational tools to explain the behaviour of connection between steel and concrete. Nonlinear simulation using the models in ATENA can be efficiently used to support and extend experimental investigations and to predict behaviour of structures and structural details. Several constitutive models covering these effects are implemented in the computer code ATENA, which is a finite element package designed for computer simulation of concrete structures. The graphical user interface in ATENA provides an efficient and powerful environment for solving many anchoring problems. ATENA enables virtual testing of structures

using computers, which is the present trend in the research and development world. Utilization of ATENA for simulation of connections between steel and concrete is good.

In ATENA, concrete is represented by solid brick element, reinforcement by bar elements and FRP by shell elements. Material properties play an important role in modeling of a structure.

3.4 MATERIAL MODELS

The program ATENA offers a variety of material models for different materials and purposes. The most important material models in ATENA for RCC structure are concrete and reinforcement. These advanced models considers all the important aspects of real material behaviour in tension and compression. GFRP material modelling is also considered.

3.4.1 Modelling of Concrete

1) Geometry of the Concrete

Element geometric modelling of concrete has been done using 3D solid brick element with 8 up to 20 nodes in ATENA, shown in Figure 3.1.

2) Element Properties

3D solid brick element having three degree of freedom at each node: translations in the nodal x, y and z directions. This is an isoparametric elements integrated by Gauss integration at integration points. This element is capable of plastic deformation, cracking in three orthogonal directions, and crushing. The most important aspect of this element is the treatment of non-linear material properties.

3) Element Interpolation function

3D solid brick element interpolation functions for all variants of the elements are given below:

N1= (1/8) (1+r) (1+s) (1+t) N2= (1/8) (1-r) (1+s) (1+t)

N3= (1/8) (1-r) (1-s) (1+t) N4= (1/8) (1+r) (1-s) (1+t)

N5= (1/8) (1+r) (1+s) (1-t) N6= (1/8) (1-r) (1+s) (1-t)

N7= (1/8) (1-r) (1-s) (1-t) N8= (1/8) (1+r) (1-s) (1-t)

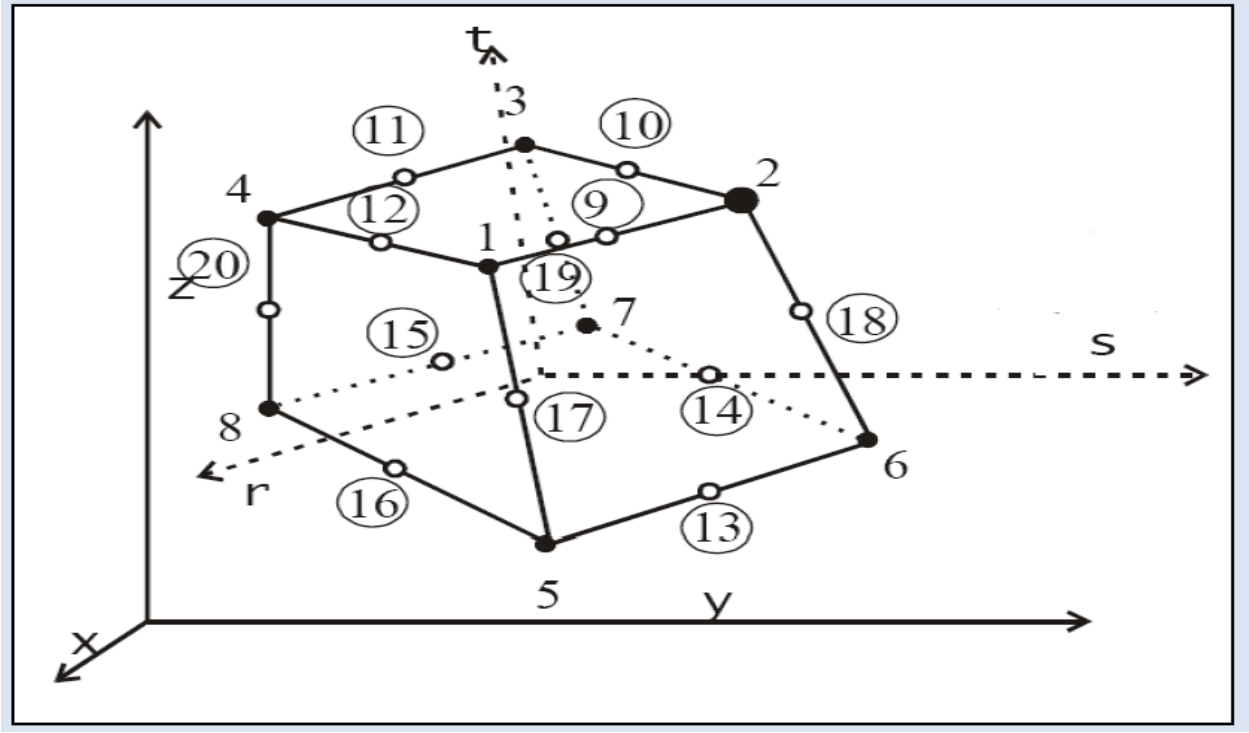

Figure 3.1 Geometry of Brick elements

3.4.2 Modelling of Reinforcement

1) Geometry of the Reinforcement

Reinforcement modelling could be discrete or smeared. In our work, a discrete modelling of reinforcement has been done. The reinforcement has been modelled using bar elements in ATENA.

2) Element Properties

Reinforcement steel is a 3D bar element, which has three degrees of freedom at each node; translations in the nodal x, y and z direction. Bar element is a uniaxial tension-compression element. The stress is assumed to be uniform over the entire element. Also plasticity, creep, swelling, large deflection and stress-stiffening capabilities are included in the element.

3) Element Shape Functions

The shape functions in natural co-ordinate system for the three dimensional bar element without rotational degrees of freedom.

N1= (1/2) (1+s) N2= (1/2) (1-s)

3.4.3 Modelling of FRP

The FRP modelling can be done as a 3D shell element in ATENA. The Ahmad shell element implemented in ATENA, described in ATENA theory manual. The present Ahmad element belongs to group of shell element formulation that is based on 3D elements concept. It can be used to model thin as well as thick shell or plate structures.

1) Geometry of the FRP

The FRP can be modelled as a shell element in ATENA. The Ahmad shell element used the 20 nodes isoparametric brick element as shown in Figure 3.2. This is needed, in order to be able to use the same pre and post-processors support for the shell and native 3D brick element. After the 1st step of the analysis, the input geometry will automatically change to the external geometry from Figure 3.2. As nodes 17 and 18 contain only so called bubble function, the element is post- processed in the same way is it would be the isoparametric brick element. Internally, all element's vectors and matrices are derived based on the internal geometry as depicted also shown in Figure 3.2.

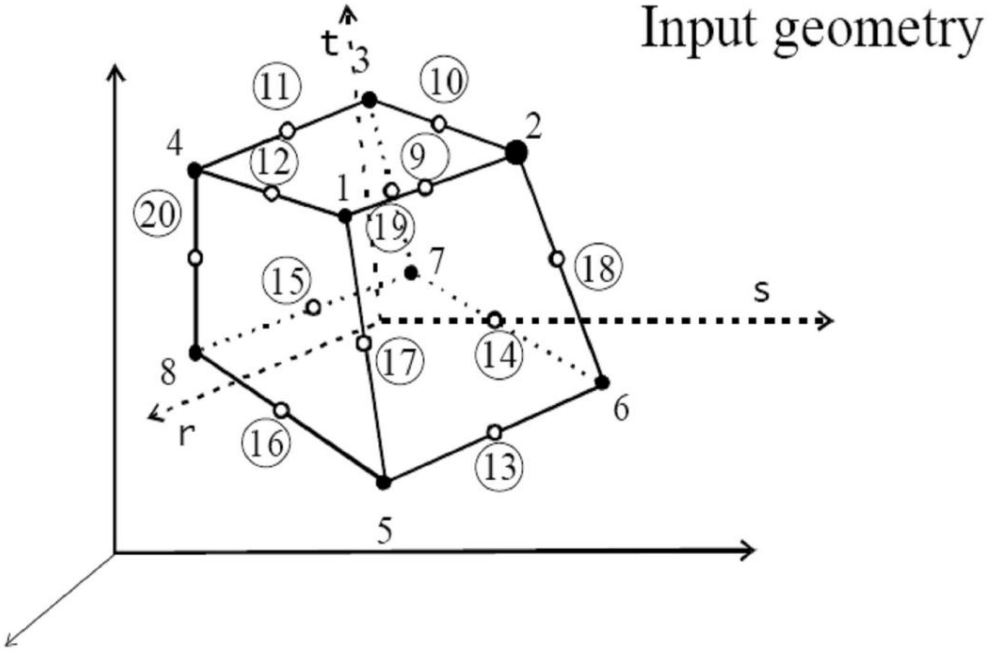

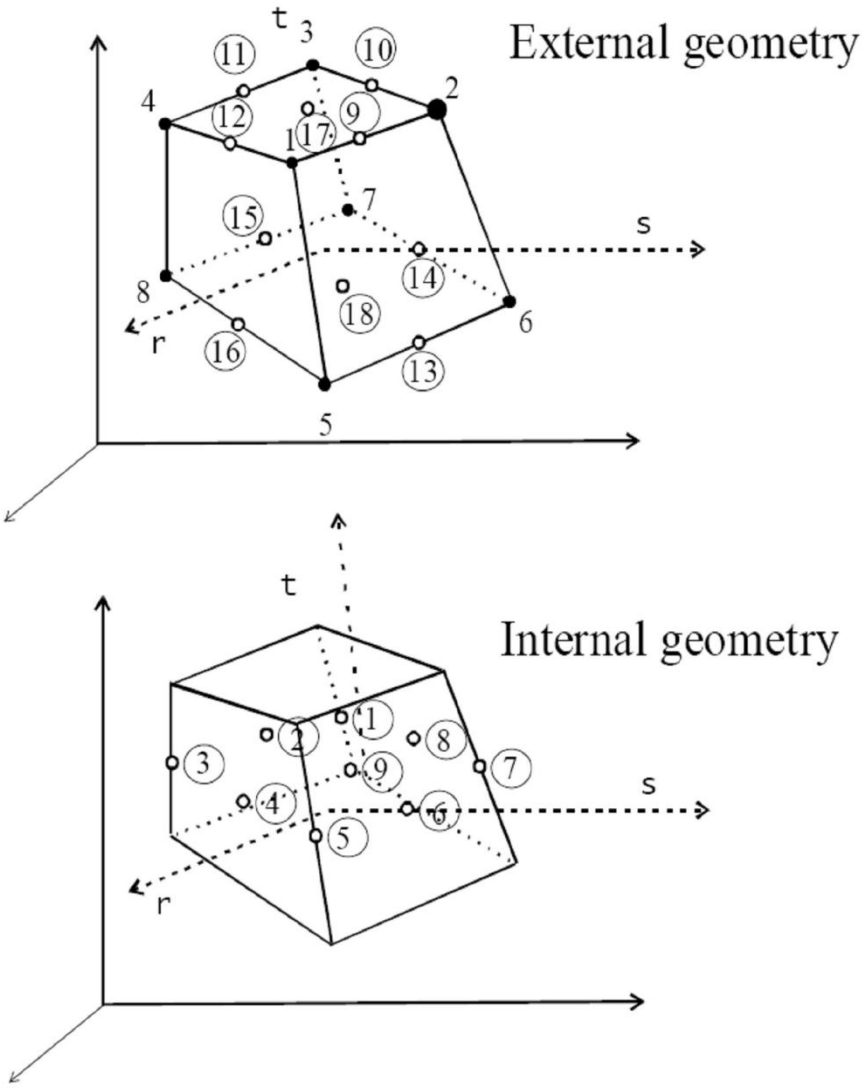

Figure 3.2 Geometry of the FRP

2) Element property of the FRP

FRP is a Ahmad shell element. In the following general shell element theory concept, every node of element has five degree of freedom, e.g. three displacements and two rotations in planes normal to mid surface of element. In order to facilitate a simple connection of this element with other true 3D elements, the (original) five degrees of freedom are transformed into x, y, z displacement of a top node and x, y displacement of a bottom node degrees of freedom. The two nodes are located on the normal to mid-surface passing thru the original mid-surface element's node.

3.5 STRESS - STRAIN RELATIONS FOR CONCRETE [20]

Concrete exhibits a large number of micro-cracks, especially, at the interface between coarser aggregates and mortar, even before subjected to any load. The presence of these micro-cracks has a great effect on the mechanical behaviour of concrete, since their propagation during loading contributes to the nonlinear behaviour at low stress levels and causes volume expansion near failure. Many of these micro-cracks are caused by segregation, shrinkage or thermal expansion of the mortar. Some micro-cracks may develop during loading because of the difference in stiffness between aggregates and mortar. Since the aggregate-mortar interface has a significantly lower tensile strength than mortar, it constitutes the weakest link in the composite system. This is the primary reason for the low tensile strength of concrete.

The response of a structure under load depends to a large extent on the stress-strain relation of the constituent materials and the magnitude of stress. Since concrete is used mostly in compression, the **stress-strain relation** in compression is of primary interest [20].

3.5.1 Equivalent Uniaxial Law

The nonlinear behaviour of concrete in the biaxial stress state is described by means of the so called effective stress σ_c^{ef}, and the equivalent uni-axial strain ε^{eq}. The effective stress is in most cases a principal stress.

The equivalent uni-axial strain is introduced in order to eliminate the Poisson's effect in the plane stress state.

$$\boldsymbol{\varepsilon^{eq} = \sigma_{ci} / E_{ci}}$$

The equivalent uni-axial strain can be considered as the strain, that would be produced by the stress σ_{ci} in a uni-axial test with modulus associated E_{ci} with the direction i. Within this assumption, the nonlinearity representing damage is caused only by the governing stress σ_{ci}. The complete equivalent uni-axial stress-strain diagram for concrete is shown in Figure 3.3.

The numbers of the diagram parts in Figure 3.3 (material state numbers) are used in the results of the analysis to indicate the state of damage of concrete.

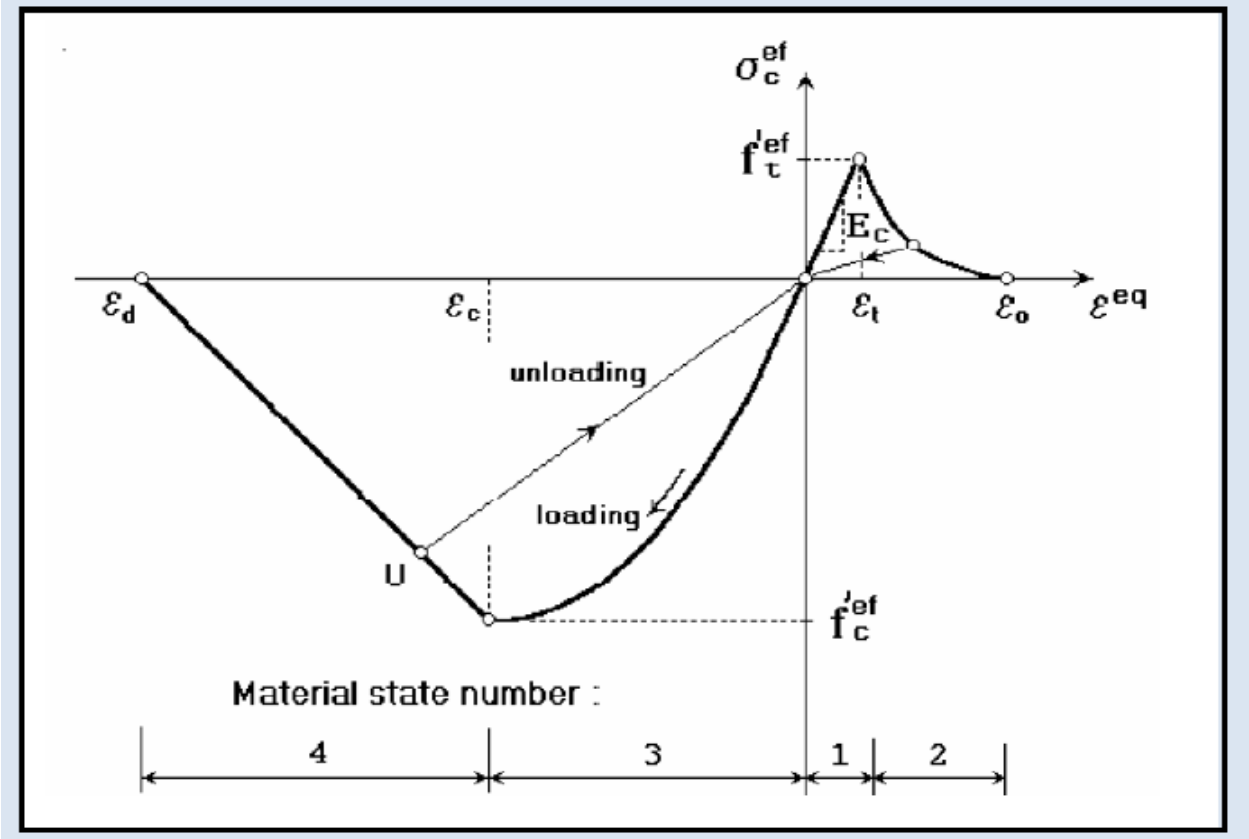

Figure 3.3 Uniaxial stress-strain law for concrete [20]

Unloading is a linear function to the origin. An example of the unloading point U is shown in Figure 3.3. Thus, the relation between stress σ_c^{ef} and strain ε^{eq} is not unique and depends on a load history. A change from loading to unloading occurs, when the increment of the effective strain changes the sign. If subsequent reloading occurs the linear unloading path is followed until the last loading point U is reached again. Then, the loading function is resumed.

The peak values of stress in compression f_c^{ef} and in tension f_t^{ef} are calculated according to the biaxial stress state. Thus, the equivalent uni-axial stress-strain law reflects the biaxial stress state

3.5.2 Biaxial stress failure criterion of concrete

1) Compressive Failure

A biaxial stress failure criterion according to KUPFER et al. (1969) is used as shown in **Figure3.4**. In the compression-compression stress state the failure function is

$$\mathbf{f'_c{}^{ef} = [(1+3.65a)/(1+a)2]f'_c;\ \ a = (\sigma_{c1}/\sigma_{c2})} \qquad (3.1)$$

where,

σ_{c1}, σ_{c2} are the principal stresses in concrete and

f_c is the uni-axial cylinder strength.

In the biaxial stress state, the strength of concrete is predicted under the assumption of a proportional stress path.

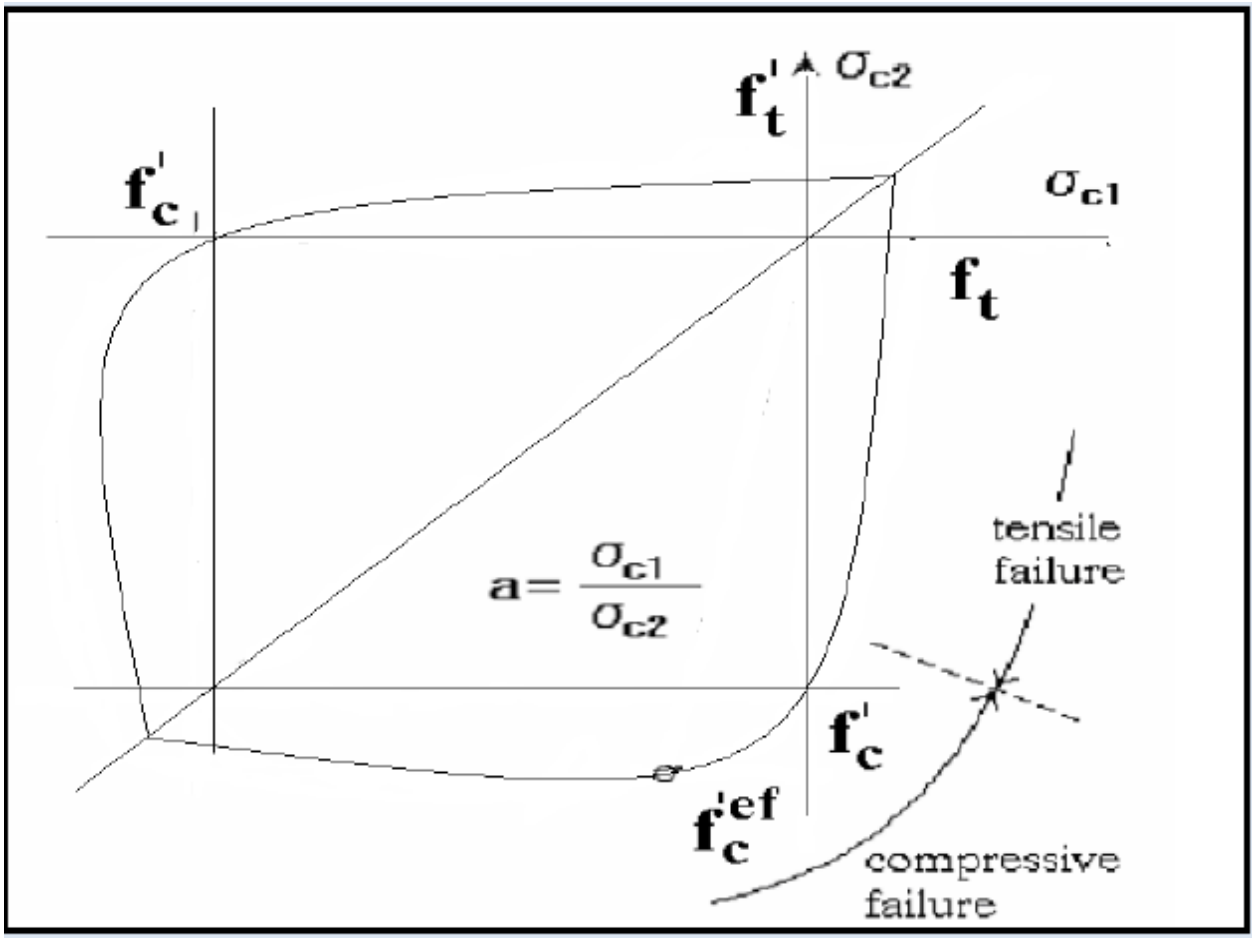

Figure 3.4 Biaxial failure functions for concrete [20]

In the tension-compression state, the failure function continues linearly from the point $\sigma_{c1} = 0$, $\sigma_{c2} = f'_c$, into the tension-compression region with the linearly decreasing strength:

$$f'^{ef}_c = f'_c\, r_{ec}, \qquad r_{ec} = [1 + 5.3278(\sigma_{c1}/ f'_c)] \tag{3.2}$$

where r_{ec} is the reduction factor of the compressive strength in the principal direction 2 due to the tensile stress in the principal direction 1.

2) Tensile failures

In the tension-tension state, the tensile strength is constant and equal to the uniaxial tensile strength f'_t. In the tension-compression state, the tensile strength is reduced by the relation:

$$\mathbf{f'^{ef}_t = f'_t\, r_{et}} \tag{3.3}$$

Where r_{et} is the reduction factor of the tensile strength in the direction 1 due to the compressive stress in the direction 2. The reduction function has one of the following forms, fig.3.5.

$$\mathbf{r_{et} = 1 - 0.8\,(\sigma_{c2}/\, f'_c)} \tag{3.4}$$

$$\mathbf{r_{et} = [A + (A - 1)\,B]/\, AB;\; B = Kx + A;\; x = \sigma_{c2}/\, f'_c} \tag{3.5}$$

The relation in eq. (3.4) represents the linear decrease of the tensile strength and eq. (3.5) represents the hyperbolic decrease.

Two predefined shapes of the hyperbola are given by the position of an intermediate point r, x. Constants K and A define the shape of the hyperbola. The values of the constants for the two positions of the intermediate point are given in the following table.

Type	*Point*		*Parameters*	
	r	X	A	K
A	0.5	0.4	0.75	1.125
B	0.5	0.2	1.0625	6.0208

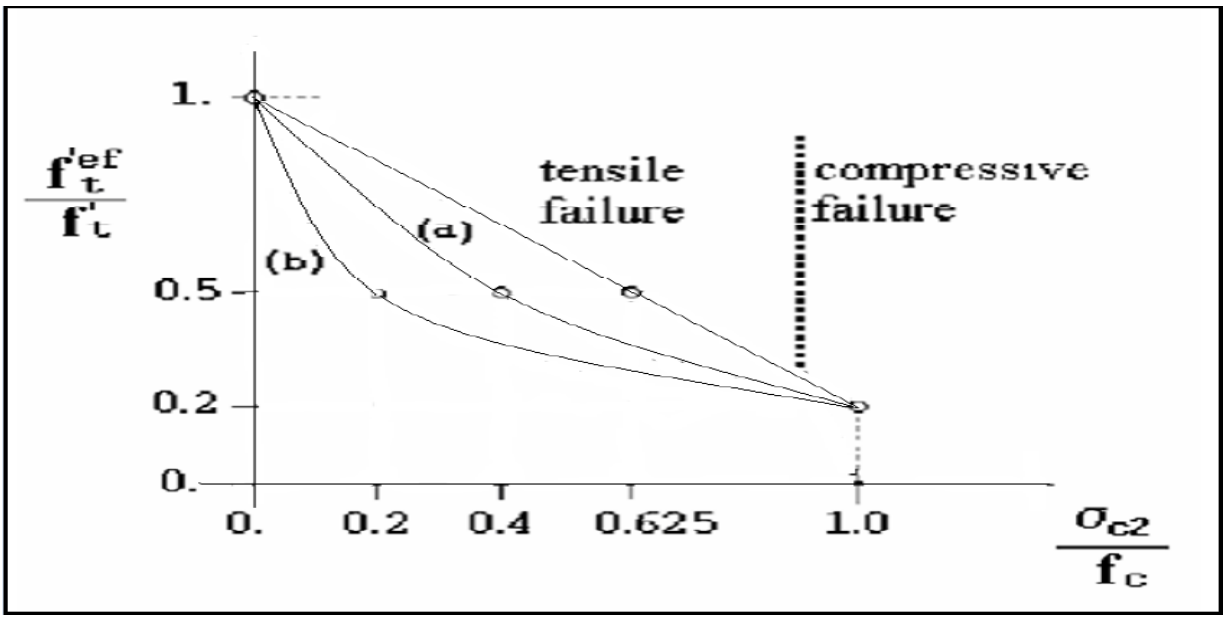

Figure 3.5 Tension Compression failure function of concrete [20]

3.5.3 Tension before cracking

The behaviour of concrete in tension without cracks is assumed linear elastic. E_c is the initial elastic modulus of concrete, f'^{ef}_t is the effective tensile strength derived from the biaxial failure function already describe above.

$$\sigma_c^{ef} = E_c\, \varepsilon^{eq},\ 0 < \sigma_c < f'^{ef}_t$$

3.5.4 Tension after cracking

A fictitious crack model is based on a crack-opening law and fracture energy. This formulation is suitable for modelling of crack propagation in concrete. It is used in combination with the crack band. It is a region (band) of material, which represents a discrete failure plane in the finite element analysis. In tension it is a crack, in compression it is a plane of crushing. In reality these failure regions have some dimension. However, since according to the experiments, the dimensions of the failure regions are independent on the structural size, they are assumed as fictitious planes. In case of tensile cracks, this approach is known as rack the "crack band theory**", (BAZANT OH 1983).** Here is the same concept used also for the compression failure. The purpose of the failure band is to eliminate two deficiencies, which occur in connection with the application of the finite element model: element size effect and element orientation effect.

1) Element size effect.

The direction of the failure planes is assumed to be normal to the principal stresses in tension and compression, respectively. The failure bands (for tension L_t and for compression L_c) are defined as projections of the finite element dimensions on the failure planes.

2) Element Orientation Effect.

The element orientation effect is reduced, by further increasing of the failure band for skew meshes, by the following formula (proposed by (**CERVENKA et al. 1995).**

$$\mathbf{L_t = \gamma L_t, L_c = \gamma L_c}$$

$$\gamma = 1 + (\gamma^{max} - 1)\,(\theta/45),\ \theta\ \varepsilon\ (0; 45) \qquad (3.6)$$

An angle θ is the minimal angle (min (θ_1, θ_2)) between the direction of the normal to the failure plane and element sides. In case of a general quadrilateral element the element sides' directions are calculated as average side directions for the two opposite edges. The above formula is a linear interpolation between the factor γ=1.0 for the direction parallel with element sides, and $\gamma=\gamma^{max}$, for the direction inclined at 45o. The recommended (and default) value of γ^{max} =1.5.

3.6 BEHAVIOUR OF CRACKED CONCRETE [20]

3.6.1 Description of a cracked section

The nonlinear response of concrete is often dominated by progressive cracking which results in localized failure. The structural member has cracked at discrete locations where the concrete tensile strength is exceeded.

At the cracked section all tension is carried by the steel reinforcement. Tensile stresses are, however, present in the concrete between the cracks, since some tension is transferred from steel to concrete through bond. The magnitude and distribution of bond stresses between the cracks determines the distribution of tensile stresses in the concrete and the reinforcing steel between the cracks.

Additional cracks can form between the initial cracks, if the tensile stress exceeds the concrete tensile strength between previously formed cracks. The final cracking state is reached when a

tensile force of sufficient magnitude to form an additional crack between two existing cracks can no longer be transferred by bond from steel to concrete.

As the concrete reaches its tensile strength, primary cracks form. The number and the extent of cracks are controlled by the size and placement of the reinforcing steel. At the primary cracks the concrete stress drops to zero and the steel carries the entire tensile force. The concrete between the cracks, however, still carries some tensile stress, which decreases with increasing load magnitude. This drop in concrete tensile stress with increasing load is associated with the breakdown of bond between reinforcing steel and concrete. At this stage a secondary system of internal cracks, called bond cracks, develops around the reinforcing steel, which begins to slip relative to the surrounding concrete.

Since cracking is the major source of material nonlinearity in the serviceability range of reinforced concrete structures, realistic cracking models need to be developed in order to accurately predict the load-deformation behaviour of reinforced concrete members. The selection of a cracking model depends on the purpose of the finite element analysis. If overall load-deflection behaviour is of primary interest, without much concern for crack patterns and estimation of local stresses, the "smeared" crack model is probably the best choice. If detailed local behaviour is of interest, the adoption of a "discrete" crack model might be necessary. Unless special connecting elements and double nodes are introduced in the finite element discretization of the structure, the well established smeared crack model results in perfect bond between steel and concrete, because of the inherent continuity of the displacement field.

3.6.2 Modelling of cracks in concrete

The process of crack formation can be divided into three stages, Figure 3.6. The un-cracked stage is before a tensile strength is reached. The crack formation takes place in the process zone of a potential crack with decreasing tensile stress on a crack face due to a bridging effect. Finally, after a complete release of the stress, the crack opening continues without the stress.

The tension failure of concrete is characterized by a gradual growth of cracks, which join together and eventually disconnect larger parts of the structure. It is usually assumed that cracking formation is a brittle process and that the strength in tension loading direction abruptly goes to zero after such cracks have formed.

Therefore, the formation of cracks is undoubtedly one of the most important non-linear phenomenon, which governs the behaviour of the concrete structures. In the finite element analysis of concrete structures, two principally different approaches have been employed for crack modelling. These are (a) discrete crack modelling (b) smeared crack modeling.

The discrete approach is physically attractive but this approach suffers from few drawbacks, such as**,** it employs a continuous change in nodal connectivity, which does not fit in the nature of finite element displacement method; the crack is considered to follow a predefined path along the element edges and excessive computational efforts are required. The second approach is the smeared crack approach. In this approach the cracks are assumed to be smeared out in a continuous fashion.

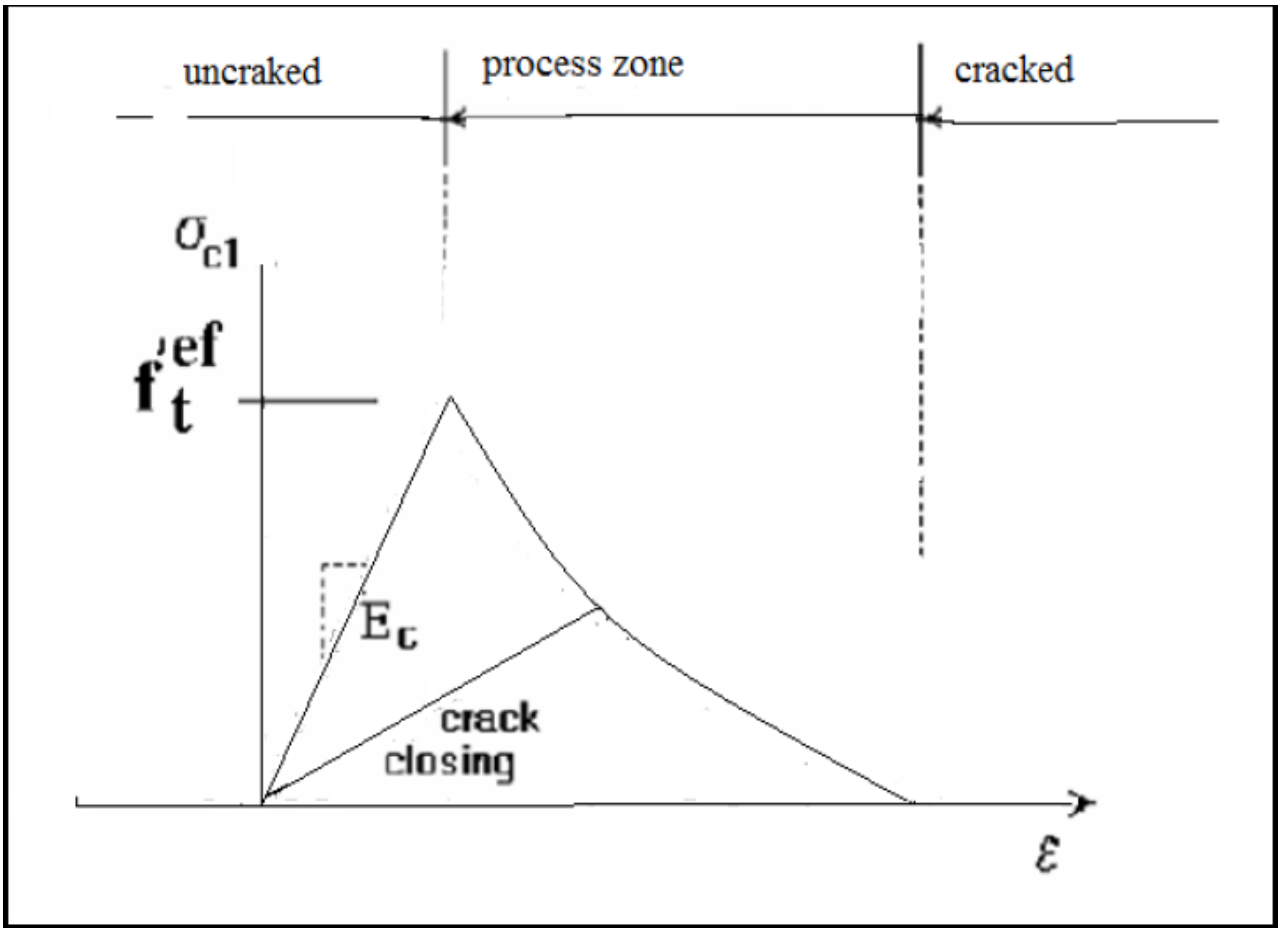

Figure 3.6 Stages of Crack Opening [20]

Within the smeared concept two options are available for crack models: the fixed crack model and the rotated crack model. In both models the crack is formed when the principal stress exceeds the tensile strength. It is assumed that the cracks are uniformly distributed within the material volume. This is reflected in the constitutive model by an introduction of orthotropy.

1) Fixed Crack Model

In the fixed crack model (**CERVENKA 1985, DARWIN 1974**) the crack direction is given by the principal stress direction at the moment of the crack initiation. During further loading this direction is fixed and represents the material axis of the orthotropy.

The principal stress and strain directions coincide in the un-cracked concrete, because of the assumption of isotropy in the concrete component. After cracking the orthotropy is introduced. The weak material axis m_1 is normal to the crack direction; the strong axis m_2 is parallel with the cracks. In a general case the principal strain axes ε_1 and ε_2 rotate and need not to coincide with the axes of the orthotropy m_1 and m_2. This produces a shear stress on the crack face as shown in Figure. 3.7. The stress components σ_{c1} and σ_{c2} denote, respectively, the stresses normal and parallel to the crack plane and, due to shear stress, they are not the principal stresses.

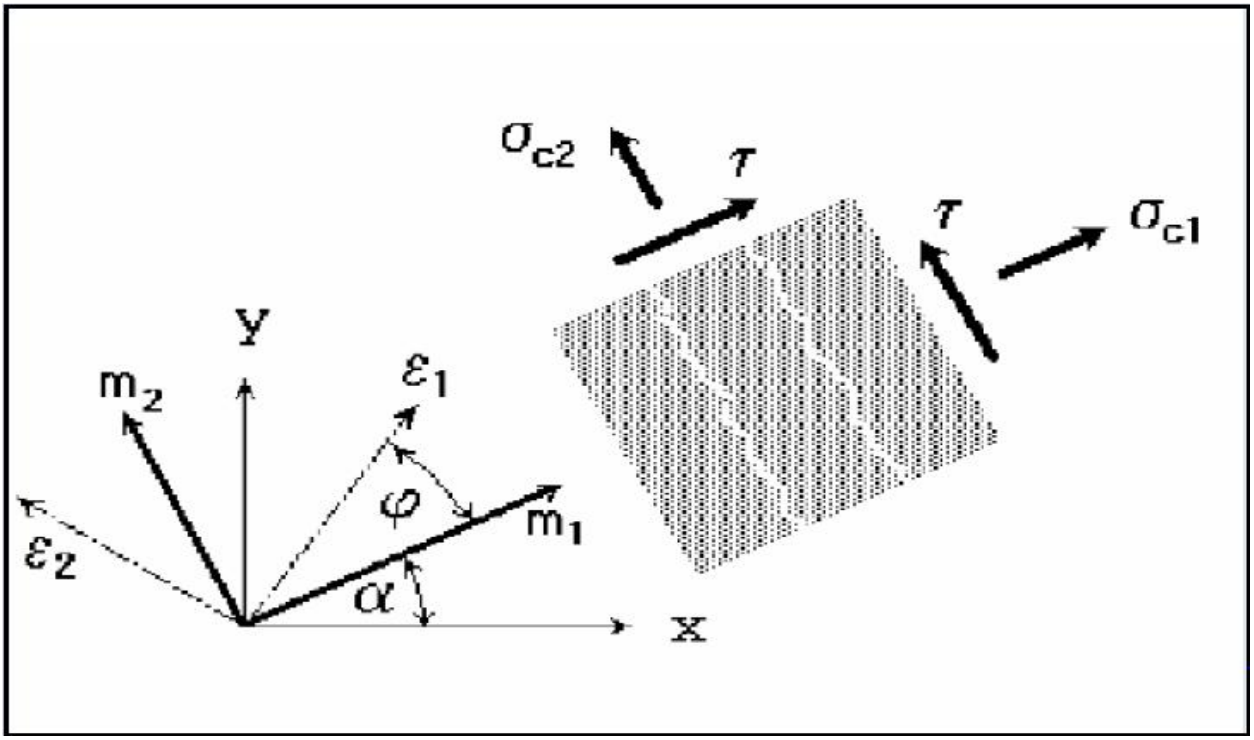

Figure 3.7 Fixed crack model Stress and strain state [20]

2) Rotated Crack Model

In the rotated crack model, the direction of the principal stress coincides with the direction of the principal strain. Thus, no shear strain occurs on the crack plane and only two normal stress components must be defined, as shown in Figure 3.8.

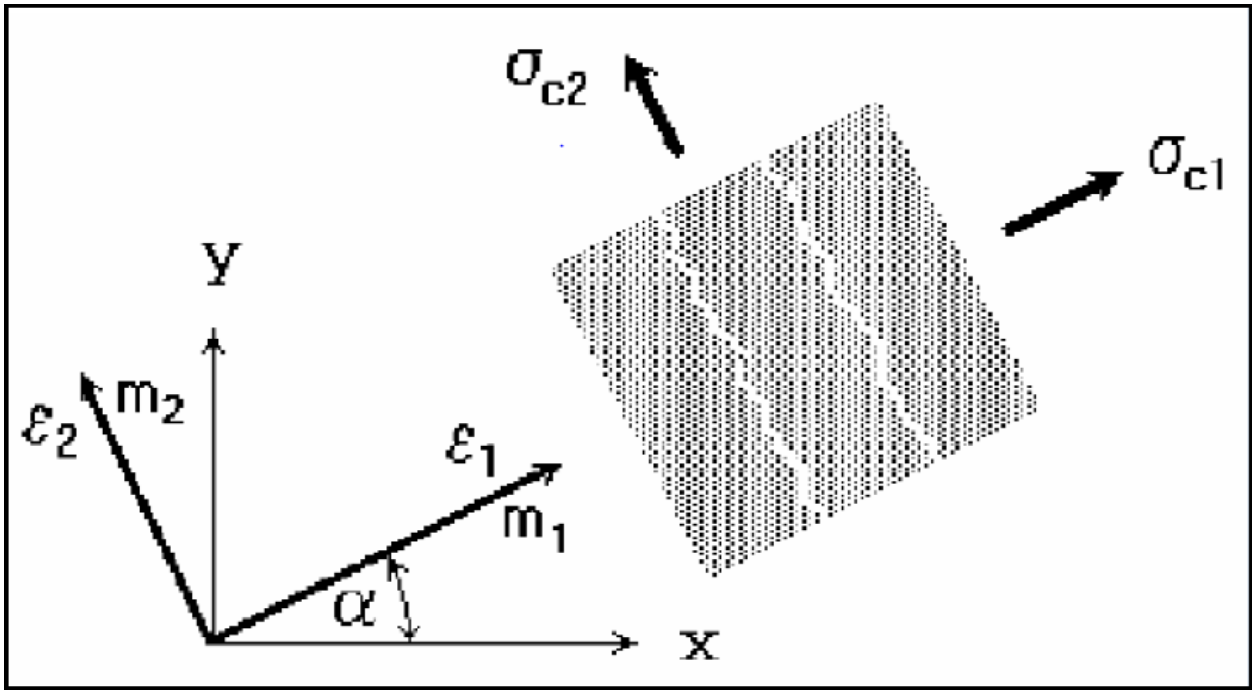

Figure 3.8 Rotated crack model. Stress and strain state [20]

If the principal strain axes rotate during the loading the direction of the cracks rotates, too. In order to ensure the co-axiality of the principal strain axes with the material axes the tangent shear modulus Gt is calculated according to CRISFIELD 1989 as

$$G_t = (\sigma_{c1} - \sigma_{c2}) / 2\,(\varepsilon_1 - \varepsilon_2)$$

3.7 STRESS-STRAIN LAWS FOR REINFORCEMENT [20]

3.7.1 Introduction

Reinforcement can be modelled in two distinct forms: discrete and smeared. Discrete reinforcement is in form of reinforcing bars and is modelled by truss elements. The smeared

reinforcement is a component of composite material and can be considered either as a single (only one-constituent) material in the element under consideration or as one of the more such constituents. The former case can be a special mesh element (layer), while the later can be an element with concrete containing one or more reinforcements. In both cases the state of uniaxial stress is assumed and the same formulation of stress-strain law is used in all types of reinforcement.

3.7.2 Bilinear Law

The bilinear law, elastic-perfectly plastic, is assumed as shown in Figure 3.9

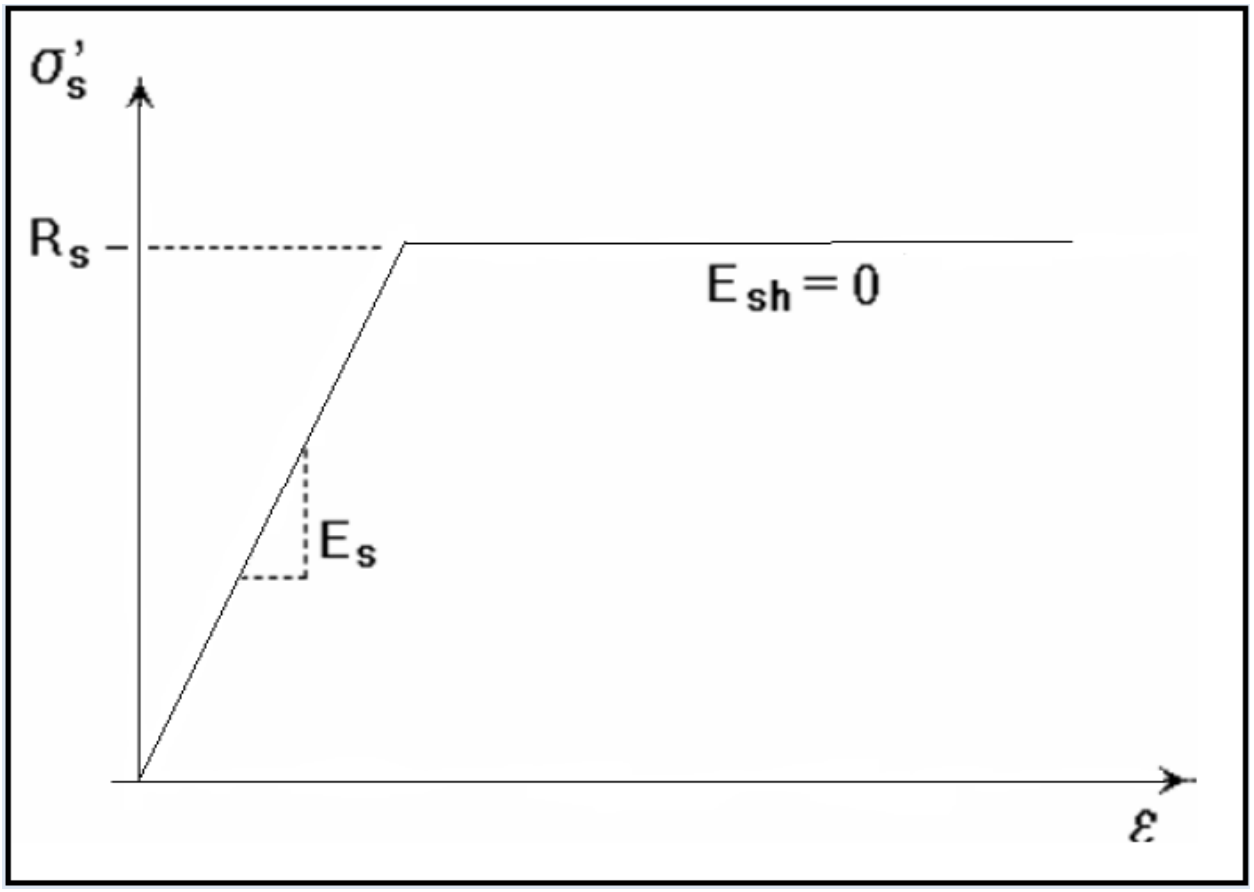

Figure 3.9 The bilinear stress-strain law for reinforcement [20]

The initial elastic part has the elastic modulus of steel E_s. The second line represents the plasticity of the steel with hardening and its slope is the hardening modulus E_{sh}. In case of perfect plasticity E_{sh} =0. Limit strain ε_L represents limited ductility of steel.

3.7.3 Multi-linear Law

The multi-linear law consists of four lines as shown in Figure 3.10. This law allows modelling of all four stages of steel behaviour: elastic state, yield plateau, hardening and fracture. The multi-line is defined by four points, which can be specified by input.

The above described stress-strain laws can be used for the discrete as well as the smeared reinforcement. The smeared reinforcement requires two additional parameters: the reinforcing ratio p and the direction angle β as shown in Figure 3.11.

Where ρ = (Area of steel/ Area of concrete)

The spacing s of the smeared reinforcement is assumed infinitely small. The stress in the smeared reinforcement is evaluated in the cracks; therefore it should include also a part of stress due to tension stiffening.

$$\sigma_{scr} = \sigma_s + \sigma_{ts}$$

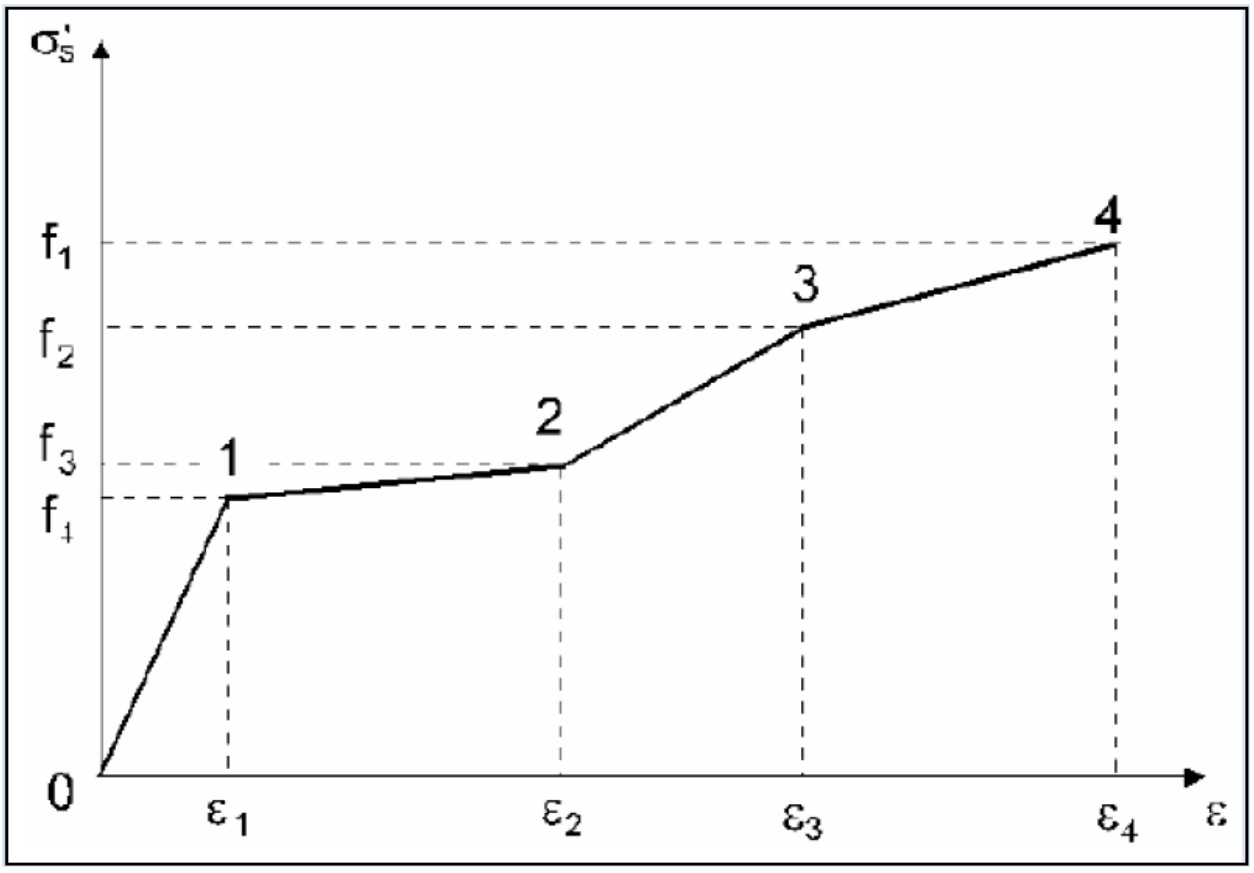

Figure 3.10 The multi-linear stress-strain law for reinforcement [20]

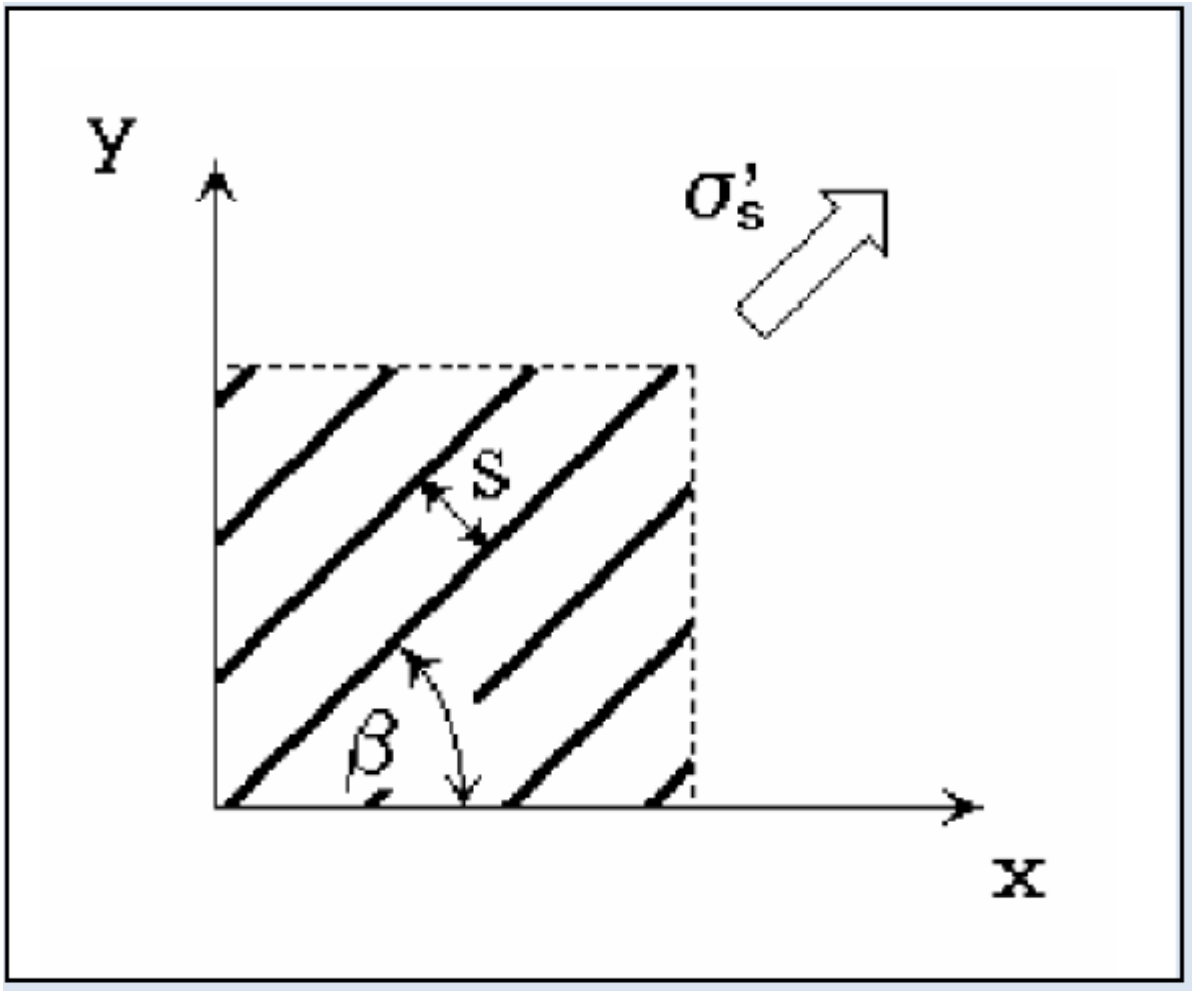

Figure3.11 Smeared reinforcement [20]

where, σ_s is the steel stress between the cracks (the steel stress in smeared reinforcement), σ_{scr} is the steel stress in a crack. If no tension stiffening is specified $\sigma_{ts} = 0$ and $\sigma_{scr} = \sigma_s$. In case of the discrete reinforcement the steel stress is always σ_s.

Once we understand the finite element modelling, the next step is the analytical programming. The main objective of this analytical program is to get the result of under reinforced concrete slab and compare with the experimental results. In the analytical programming, first we select the materials and its properties and create geometry of the slab. For this, four slabs are created and FE modelling is done through automatic FE mesh generator in ATENA. Out of these slabs, one slab was taken as a control slab, one as retrofitted slab and the remaining two slabs were taken as stressed retrofitted slabs to 75% and 90%. All slabs were tested up to its failure point and the ultimate load deflection values are plotted as graphs. For modelling the control and

retrofitted members in ATENA, concrete, reinforcement bars of different diameters, steel plates, epoxy and GFRP are used as materials.

3.8 MATERIAL PROPERTIES

Concrete, reinforcement steel, steel plates, Epoxy and GFRP have been used to model the RCC slab. The specification and the properties of these materials are as under:

1) Concrete

In ATENA, concrete material is modelled as a 3D nonlinear cementitious2. The physical properties of 3D nonlinear cementitious2 material are given in Table 3.1. The values are calculated as per IS code 456:2000 and remaining are the default values.

Table 3.1 Material Properties of Concrete

Properties	Values
Elastic Modulus (Fresh concrete)	25,000 MPa
Elastic Modulus (75% stressed concrete)	16250 MPa
Elastic Modulus (90% stressed concrete)	12500 MPa
Poisson Ratio	0.2
Tensile Strength	3.5 MPa
Compressive Strength	25 MPa
Specific Fracture Energy	5.130E-05 MN/m
Critical Compressive Displacement	5E-04 m
Plastic Strain at Compressive Strength	7.572E-04
Reduction of Compressive Strength	0.8
Fail Surface Eccentricity	0.52
Specific Material Weight	0.024 MN/mE+3
Coefficient of Thermal Expansion	1.20E-05 1/K
Fixed Crack Model Coefficient	1

2) Reinforcement Bars

Steel of grade Fe-722 of 4mm diameter are used as reinforcement. The properties of these bars are shown in Table 3.2.

Table 3.2 Material Properties of Reinforcement

Properties	Values
Elastic modulus	200000 MPa
Elastic modulus (75% stressed)	160000 MPa
Elastic modulus (90% stressed)	160000 MPa
Yield Strength	722 MPa
Ultimate Tensile Strength	807 MPa
Specific Material weight	7.850E-02 MN/mE+3
Coefficient of Thermal Expansion	1.2E-05 1/K

3) Steel Plate

The function of the steel plate in the ATENA is for support and for loading. Here, the property of steel plate is same as the reinforcement bar except its yield strength. The HYSD steel of grade Fe-415 was used for steel plate.

4) Epoxy

Mbrace saturant was used as a epoxy in the analysis. The material properties are taken from the "Watson Bowman Acme corp." company paper. The material properties of epoxy are shown in Table 3.3.

Table 3.3 Material Properties of Epoxy

Properties	Values
Elastic Modulus	3035 MPa
Poisson's Ratio	0.4
Specific Material Weight	8.00E-06 MN/mE+3
Coefficient of Thermal Expansion	1.200E-05 1/K

5. Glass Fibre Reinforcement Polymer

Mbrace G sheet EU-900 unidirectional Glass fibre sheet is used in retrofitting. The properties which are used in the modelling are taken from the Mbrace Product Data, shown in the Table 3.4.

Table 3.4 Material Properties of GFRP

Properties	Values
Strain, stress	(0,0); (0.005,390); (0.01,690) MPa
Specific Material Weight	0.0785 MN/mE+3
Coefficient of Thermal Expansion	1.200E-05 1/K

3.9 GENERAL DESCRIPTION OF THE SLAB

In the experimental program, three identical reinforced concrete slabs with nominal amount of reinforcement were cast. The slabs were under one-way condition having simple supports at 1300mm centre to centre distance. The dimension of all the three slabs was 1500mm length, 900mm width and 50mm thick. GFRP was used to strengthen the slab. Slab-1 acted as a control slab having no FRP laminates. The de-lamination of FRP was mainly due to failure of bond between concrete and FRP. So, proper bond was made between FRP and concrete using epoxy. Slab-2 at the bottom was strengthened with the GFRP laminates with the help of epoxy resin. In Slab-3 a GFRP sheet was bonded at the base using epoxy and is then anchored with the slab by bolting at 150mm centre to centre in X and Y directions throughout the slab. The above program was performed by **Chothani D.G.**

3.9.1 Material

Cement, sand, coarse aggregate and steel of good quality is required for casting the test slab specimen. GFRP was also used. Material has been used after testing in the laboratory. Details of the material used are given below.

3.9.1.1 Cement

Ordinary Portland Cement of grade 53 (as per IS:10269) has been used for casting slab specimen.

3.9.1.2 Fine aggregate

The river sand was used in concrete and the specific gravity of sand was 2.67. The sand was washed to remove any dust.

3.9.1.3 Coarse aggregate

Natural coarse aggregate of nominal size 10mm was used and the specific gravity of coarse aggregate was 2.72.

3.9.1.4 Steel

Steel rods of 4mm diameter were used as reinforcement. The proof stress of steel rods was 722MPa.

3.9.1.5 Water

Potable tap water as per IS: 456 (2000) has been used for concrete mixing and curing of test specimens.

3.9.1.6 FRP

Bidirectional GFRP sheets of 1mm thickness were used. The ultimate tensile strength of GFRP sheet in one direction was 31363.6MPa.

3.10 FE MODELLING OF RC SLAB IN ATENA

The ATENA program determines the nonlinear finite element analysis of structures and offers tools specially designed for computer simulation of concrete and reinforced concrete structural behavior.

ATENA program system consists of a solution core and several user interfaces. The solution core offers capabilities for variety of structural analysis tasks, such as: stress and failure analysis, transport of heat and humidity, time dependent problems (creep, dynamics), and their interactions. Solution core offers a wide range of 2D and 3D continuum models, libraries of finite elements, material models and solution methods. User interfaces are represent specialized on certain functions and thus one user interface need not necessarily provide access to all features of ATENA solution core. This limitation is made on order to maintain a transparent and user friendly user environment in all specific applications of ATENA.

ATENA 3D program is designed for 3D nonlinear analysis of solids with special tools for reinforced concrete structures. However, structures from other materials, such as soils, metals

etc. can be treated as well.

The program has three main functions:

A. Pre-processing

B. Run

C. Post-processing

A. **Pre-processing:** Input of geometrical objects (concrete, reinforcement, interfaces, etc.), loading and boundary conditions, meshing and solution parameters.

B. **Analysis:** It makes possible a real time monitoring of results during calculations.

C**. Post-processing:** Access to a wide range of graphical and numerical results.

Procedure:

In pre-processing window, the following steps are performed:-

Step1: Geometry of FE model is created .It has been presented in Figure 3.12.

Step2: Material properties are assigned to the various elements of the RC slab specimen.

Step3: Structural element, various supports, loadings, monitoring points and reinforcement details are defined. (Figure 3.13 & 3.14 & 3.15)

Step4: Finite element meshing parameters are given and meshing of the model is generated accordingly. (Figure 3.16)

Step5: Various analysis steps are defined. The FE non-linear analysis is done in Run window. The FE non-linear static analysis calculates the effects of steady loading conditions on a structure. A static analysis can, however, include steady inertia loads (such as gravity and rotational velocity), and time-varying loads that can be approximated as static equivalent. Static analysis is used to determine the displacements, stresses, strains, and forces in structures or components by loads.

Step6: FRP is modelled as a shell element. In this study, FRP is modelled at the bottom surface of the slab as shown in Figure 3.17

Step7: When the FE non linear static analysis is completed the, the results are shown in third part of the ATENA i.e. Post processing. The stress- strain values at every step, crack pattern and cracks propagation at every step shown help in to analyze the behaviour of the elements at every step of load deflection.

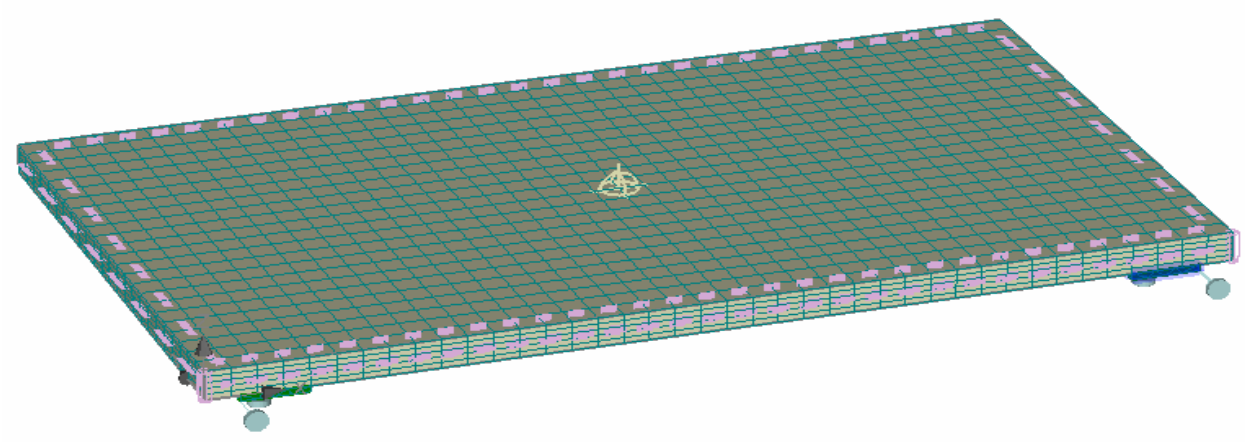

Figure 3.12 FE Model of RC Slab

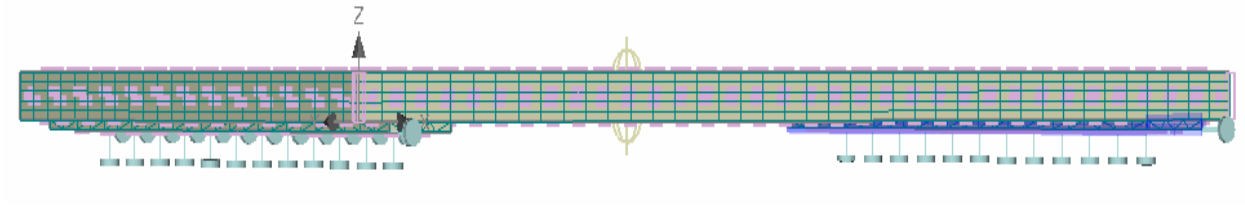

Figure 3.13 Showing supports and monitoring points

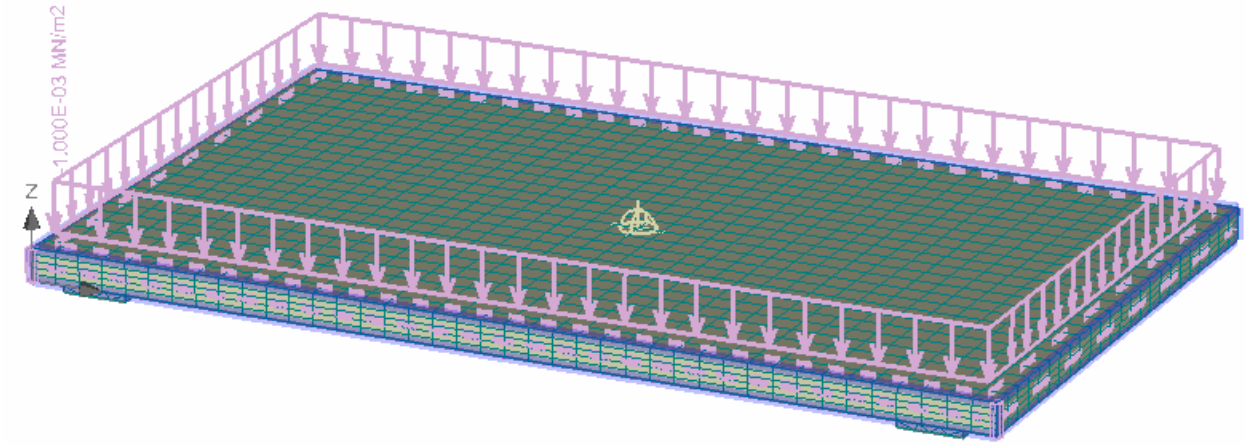

Figure 3.14 Showing area load on the slab

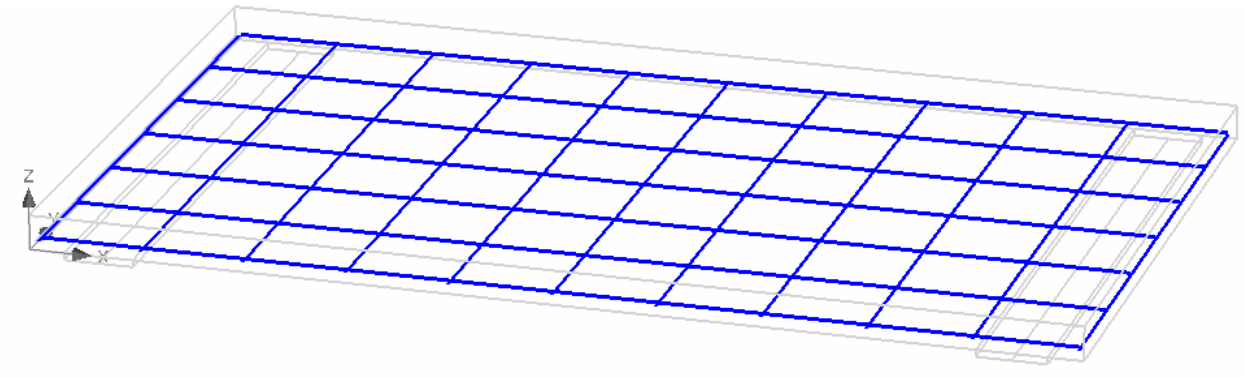

Figure 3.15 Modelling of reinforcement in the slab

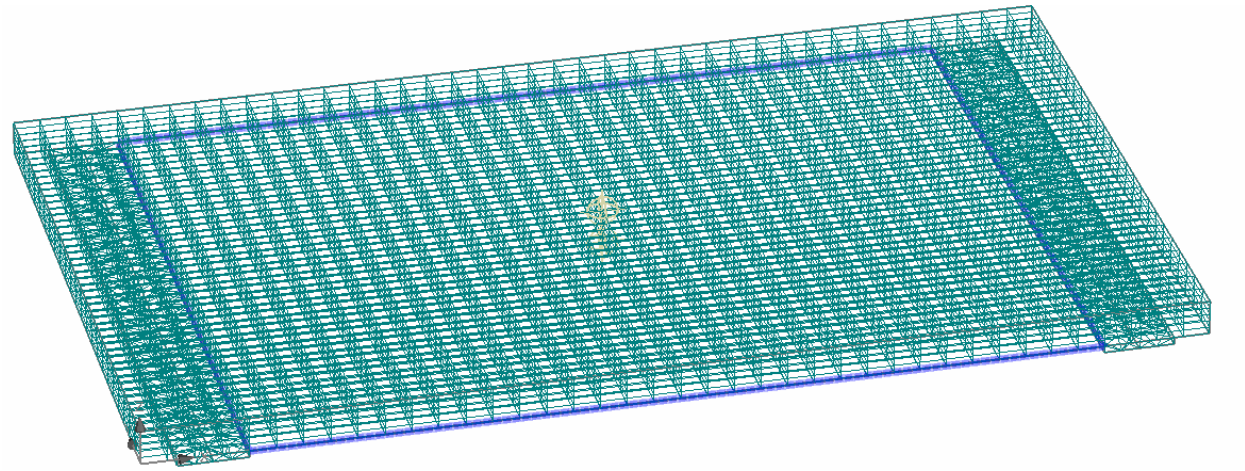

Figure 3.16 FE mesh in RC Slab

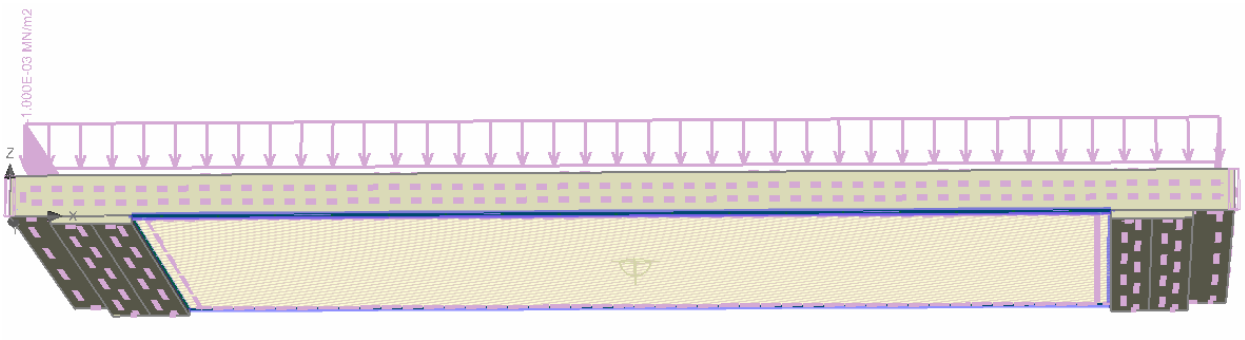

Figure 3.17 Modelling of FRP at tension face of the slab

3.11 METHODS FOR NON-LINEAR SOLUTIONS [20]

The best part of the ATENA is the simpler way of solving the non-linear structural behaviour through finite element method and its incremental loading criteria. Different methods are available in ATENA for solving non-linear equations such as, linear method, Newton-Raphson Method, Modified Newton-Raphson method, Arc Length methods are used in ATENA.

Among these the Newton-Raphson Method and Modified Newton-Raphson Method are more commonly used methods. In our present study, Newton-Raphson method is used for solving the simultaneous equations. It is an iterative process of solving the non-linear equations. One approach to non-linear solutions is to break the load into a series of load increments. The load increments can be applied either over several load steps or over several sub steps within a load step. At the completion of each incremental solution, the program adjusts the stiffness matrix to reflect the nonlinear changes in structural stiffness before proceeding to the next load increment.

The ATENA program overcomes this difficulty by using Full Newton-Raphson method, or Modified Newton-Raphson method, which drive the solution to equilibrium convergence (within some tolerance limit) at the end of each load increment. In Full Newton-Raphson method, it obtains the following set of non-linear equations:

$$K(p)\,\Delta p = q - f(p)$$

where,

q is the vector of total applied joint loads,

f(p)is the vector of internal joint forces,

Δp is the deformation increment due to loading increment,

p are the deformations of structure prior to load increment,

K(p) is the stiffness matrix, relating loading increments to deformation increments.

Figure 3.19 illustrates the use of Newton-Raphson equilibrium iterations in nonlinear analysis. Before each solution, the Newton-Raphson method evaluates the out-of -balance load vector, which is the difference between the restoring, forces (the loads corresponding to the element

stresses) and the applied loads. The program then performs a linear solution, using the out-of -balance loads, and checks for convergence. If convergence criteria are not satisfied, the out-of-balance load vector is re-evaluated, the stiffness matrix is updated, and a new solution is obtained. This iterative procedure continues until the problem converges.

But sometimes, the most time consuming part of the Full Newton-Raphson method solution is the re-calculation of the stiffness matrix K (p_i-1) at each iteration. In many cases this is not necessary and we can use matrix K (p_0) from the first iteration of the step. This is the basic idea of the so-called Modified Newton-Raphson method. It produces very significant time saving, but on the other hand, it also exhibits worse convergence of the solution procedure. The simplification adopted in the Modified Newton-Raphson method can be mathematically expressed by:

$$K(p_i-1) = K(p_0)$$

The modified Newton-Raphson method is shown in Figure 3.19. Comparing Figure3.18 and Figure3.19, it is apparent that the Modified Newton-Raphson method converges more slowly than the original Full Newton-Raphson method. On the other hand a single iteration costs less computing time, because it is necessary to assemble and eliminate the stiffness matrix only once. In practice a careful balance of the two methods is usually adopted in order to produce the best performance for a particular case. Usually, it is recommended to start a solution with the original Newton-Raphson method and later, i.e. near extreme points, switch to the modified procedure to avoid divergence.

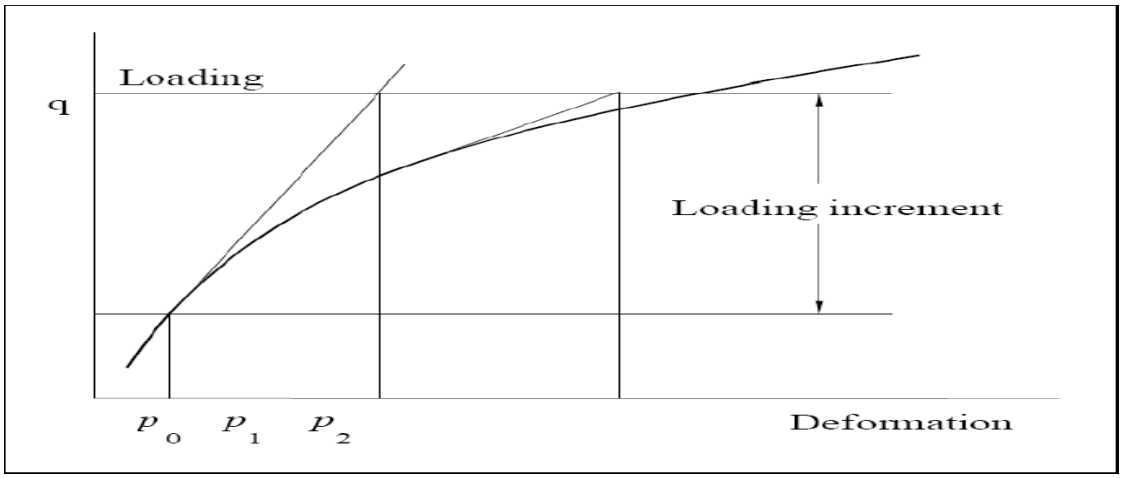

Figure 3.18 Full Newton-Raphson Method [20]

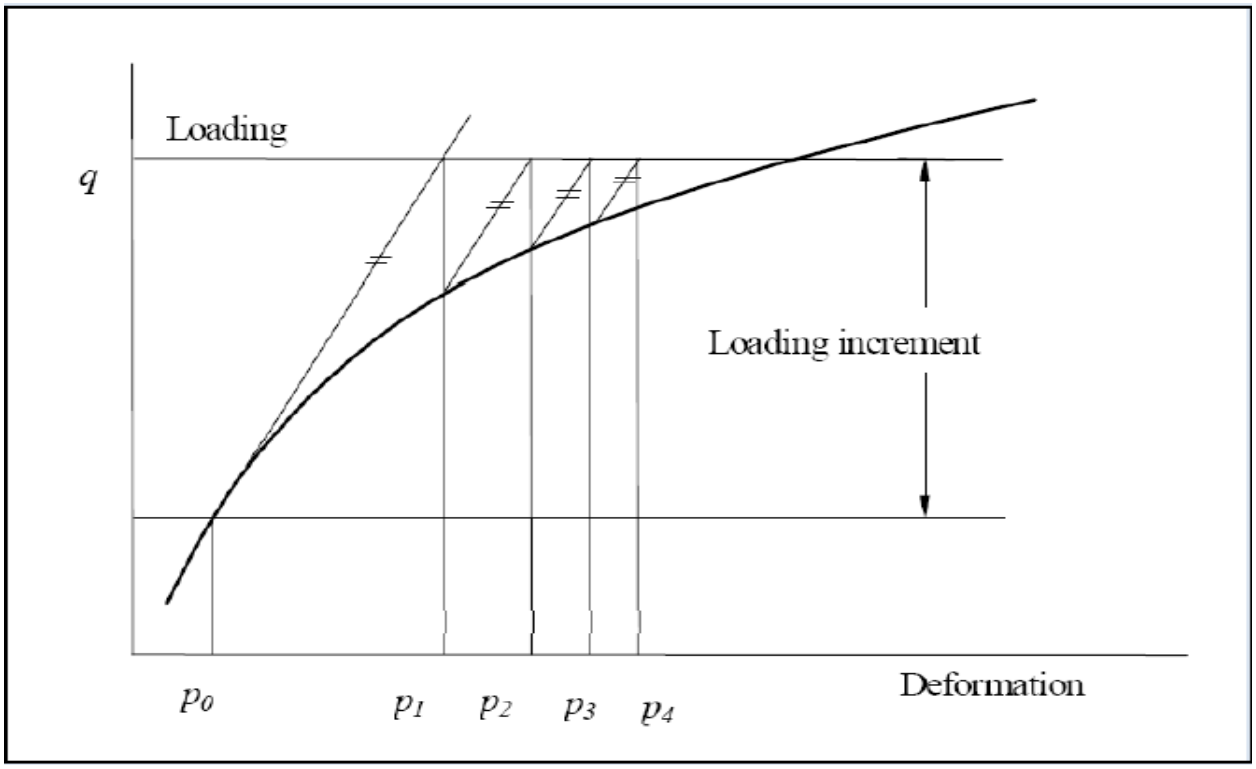

Figure 3.19 Modified Newton-Raphson Method [20]

CHAPTER 4 RESULTS AND DISCUSSIONS

4.1 GENERAL

This chapter presents the results of Finite Element analysis of control RC slab, control slab retrofitted with GFRP bonded at the bottom face. Further FE analysis of slabs stressed to 75% and 90% and then retrofitted with GFRP has been presented. Finite element analysis of RC slab under the static incremental loads has been performed in the present work. Subsequently these results are compared with experimental results. The load deflection curve and the cracking behaviour obtained from the analysis are also discussed in this chapter. In the first part, results of control slab are discussed, in the second part, results of retrofitted slab are discussed and in the third part, results of stressed retrofitted slabs are also discussed. Area load applied on the top surface of the slab has been converted to equivalent point load in analytical work because in the experimental work the point load applied is distributed on the whole surface of the slab.

4.2 FE MODEL RESULTS OF CONTROL RC SLAB

The non-linear response of RC control slab modelled as per details discussed in Chapter 3 (3.9 General Description of Structure) are presented using FE Modelling under the incremental loading. The main objective of this study is to see the variation of load- displacement graph, the crack patterns, propagation of the cracks and the crack width at different values of the loads.

In this analysis, surface load has been applied on the surface of the slab and the load is gradually increased at each step till failure. The load-deflection curves are obtained from the analysis and also the crack patterns and the width of cracks at different load levels are also observed. The size of the slab and the material properties which are used in the modelling of the control slab are same as that of the experiment performed by Chothani (2012). The characteristic performance of the control slab has been studied at each step.

4.2.1 Load v/s Deformation of the control RC slab

Results as obtained from FEM formulation in terms of load and deflection for the control RC slab are discussed here. The load-deformation curve has been plotted in Figure4.1. The load has

been increased up to its failure level and then load and deformation for all the load steps have been recorded. It is observed that the structure behaved linearly elastic up to the value of around 15.5 KN. At this point the minor cracks started appearing at the tension face of the slab. After this point the value of load decreases to 11.8 KN as the slab losses its stiffness. As the load further increases, the deflection started increasing with the load increments. When the load reached to the value of 15.5 KN, the graph depicted non-linearity in its behaviour. It is clear from the Figure4.1 that after load value of 11.8 KN, increase in deflection is more with load increments. The ultimate load carrying capacity of slab is 17.40 KN when the deflection has reached to the value of 12mm. After this point there is not much change in deflection as the load continuously decreased.

The displacements at different values of load has been tabulated in Table 4.1

Table 4.1 The load and displacement values of control slab

Load (KN)	Displacement (mm)
3	0.22
6	0.43
8.99	0.65
12	0.86
14.70	1.09
15.50	1.20
11.80	1.36
14.30	7.06
15.50	8.94
16.50	10.5
17	11.2
17.40	12.20
16.70	12.70
14	14

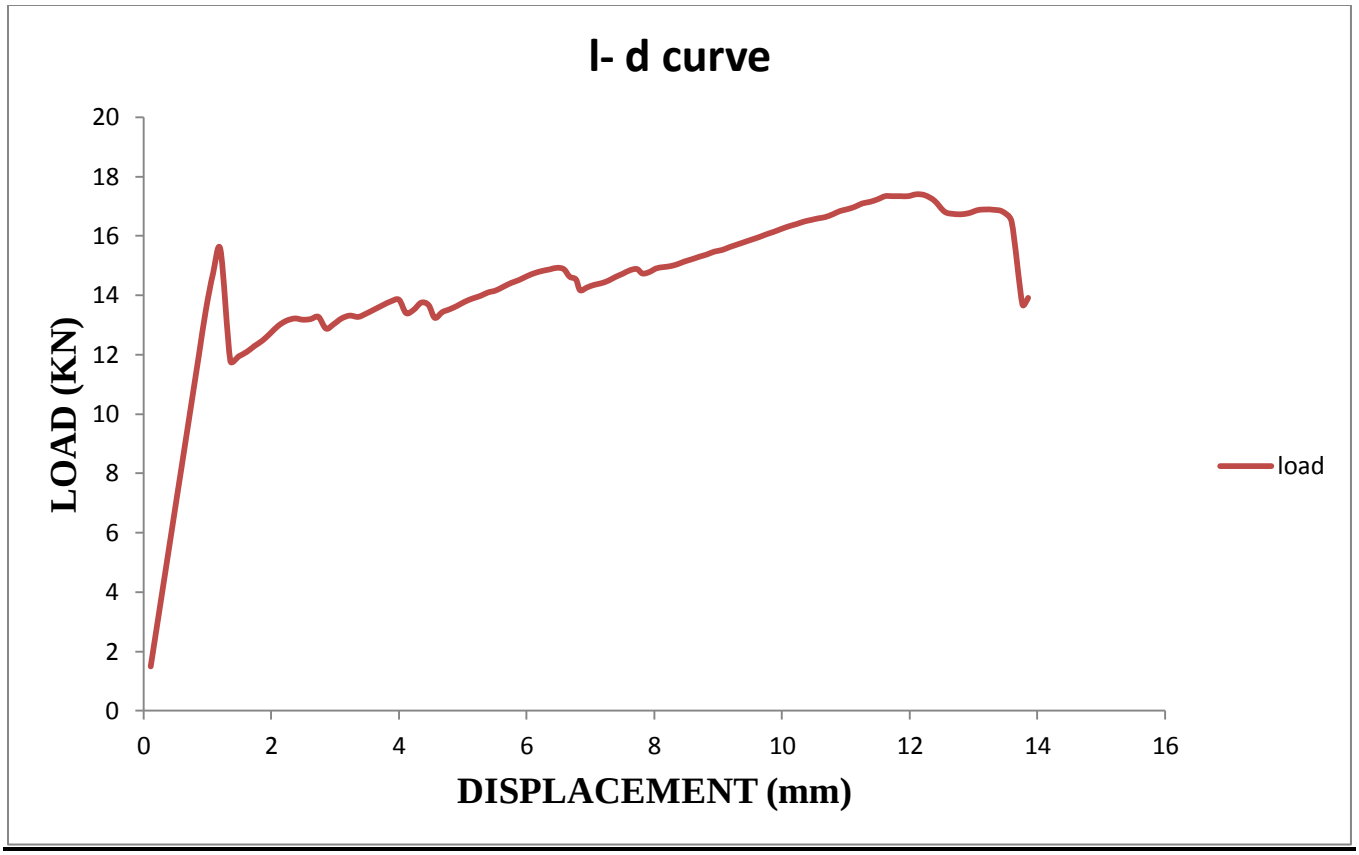

Figure 4.1 Load-Displacement curve of control RC slab

4.2.2 Crack Patterns

The variations of crack pattern due to applied load in slab are plotted in Figure 4.3-4.8 Discussions on crack patterns plotted below are presented. The shape of the deformed slab at the failure has been shown in Figure.4.2. At the early stages of loading, the behaviour of slab has been observed to be elastic until the appearance of the first crack. Invariably, the crack has been initiated at the centre of the slab and the cracks gradually propagate towards the end of the free edge on the tension face side as the loading progressed.

It has been observed that micro-cracks appeared in the structure when the slab is in linear zone. The cracks keep on increasing as the load and the deflection increases. Figure 4.3 shows that the first visible crack appeared in tension zone of slab. The maximum crack width at first peak of the curve is 0.2 mm. The first crack has been observed at load value of 15.5 KN at 1.20 mm deflection.

Figure.4.2 Deformed shape of RC slab at failure

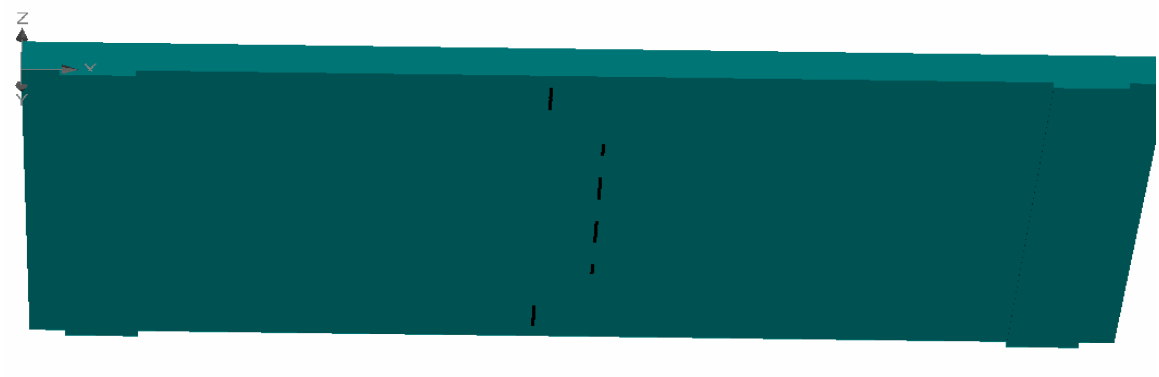

Figure.4.3 Cracks of 0.2mm width at deflection of 1.2mm

After the peak load of 15.5 KN, the value of load decreases to 11.80 KN at deflection of 1.36 mm as shown in load- deflection curve above. The crack pattern is shown in Figure 4.4. The cracks that appeared at the tension face of the slab became a bit wider and bigger. The maximum crack width at this point is 0.31 mm.

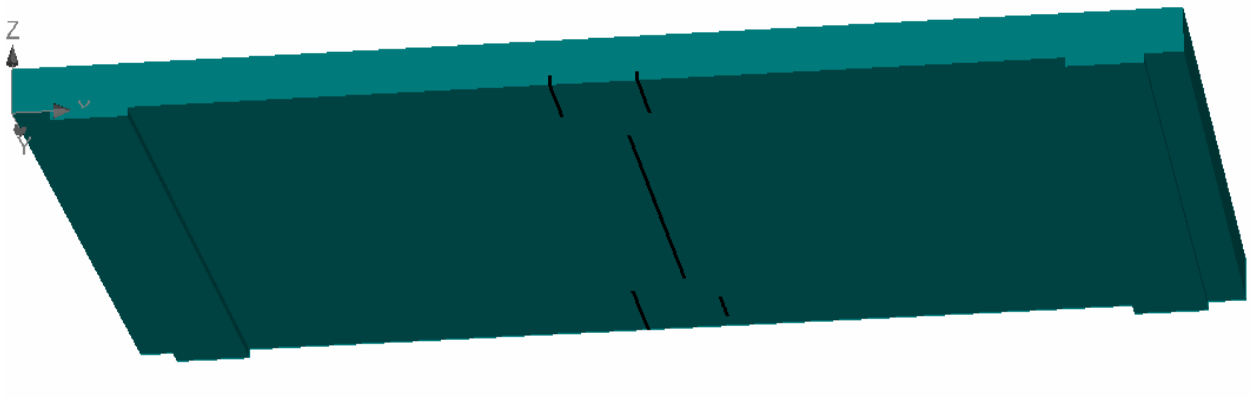

Figure.4.4 Cracks of 0.31mm width at deflection of 1.36mm

At an intermediate load step corresponding to load value of 14.3 KN cracks propagate in tension face which moves towards the free edge as shown in Figure 4.5. The displacement of 7.06mm has been observed at this stage. Flexure cracks which are observed in the tension zone of slab reduces the load carrying capacity of slab. Maximum size of crack at this load has been found to be 0.49 mm.

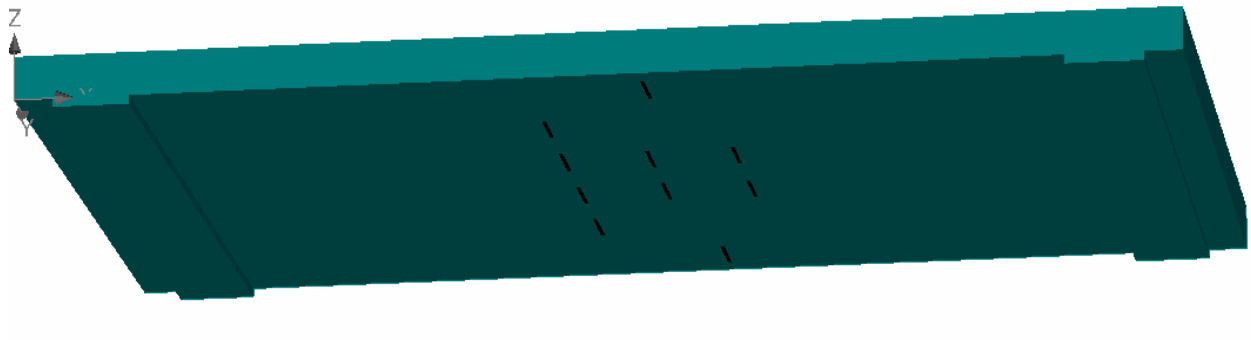

Figure.4.5 Cracks of 0.49mm width at deflection of 7.06mm

The crack pattern at maximum value of load has been described in Figure 4.6. The maximum load taken by the slab has been observed as 17.40 KN at a displacement value of 12.2 mm. The crack widens as the stiffness of slab decreases as the deflection is increasing. The maximum width of crack is 1mm.

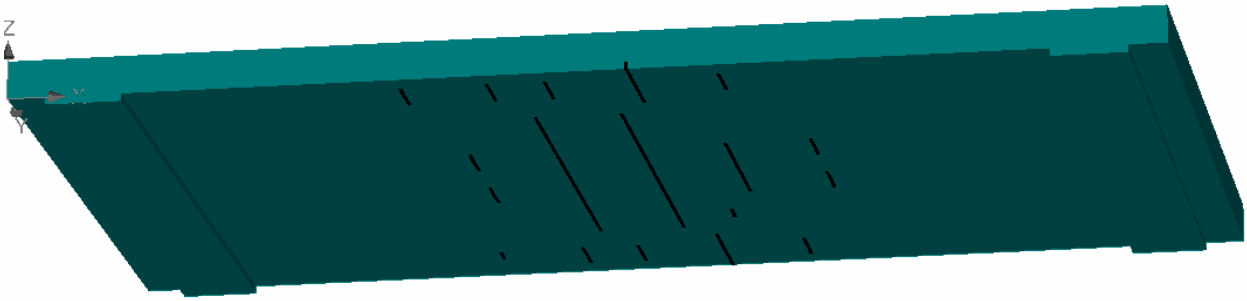

Figure.4.6 Cracks of 1mm width at deflection of 12.2mm

The crack pattern at both top and bottom has been plotted in Figure 4.7 and Figure 4.8 where maximum damage to the slab occurred**.** Major damage has been noticed at the centre of the slab while there is no damage at the corner of the slab.

Figure 4.7 All cracks at top surface of the slab at deflection of 12.2mm

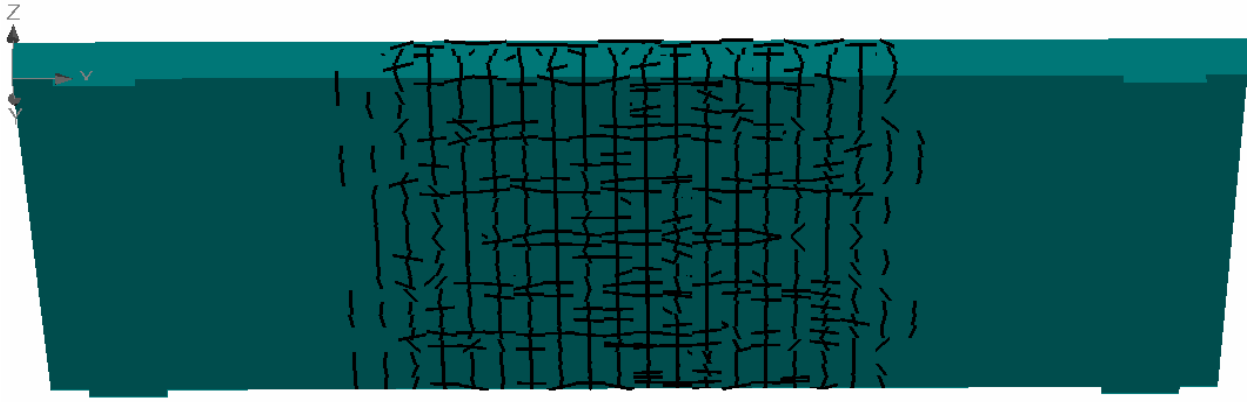

Figure 4.8 All cracks at bottom surface of the slab at deflection of 12.2mm

4.3 COMPARISON BETWEEN FE MODEL AND EXPERIMENTAL RESULTS OF THE CONTROL RC SLAB

4.3.1 Load v/s Deformation curve

The load-displacement curve plotted in Figure 4.9 shows the difference in the load carrying capacity of the slab. The result of analytical work has been compared with the experimental work done by Chothani.D.G. (2012). The ultimate load carrying capacity and maximum deflection of the slab according to experimental results was around 20 KN and 16.7mm respectively and the analytical load carrying capacity and maximum deflection has been observed to be 17.5 KN and

12.2mm respectively. The difference between the experimental and analytical values may be attributed to the choice of concrete mix grade. As in experimental work there is no mention of compressive strength of concrete, however it gives only the mix proportion. Therefore, according to the mix proportion given, grade of concrete has been considered in the analytical work. The results can very easily changed by changing the values of compressive strength. The plot depicted that initially the analytical value of load is higher than the experimental value. The behaviour of the slab has been observed to be linear up to the value of load around 15.5 KN in FE model whereas the structure has been found to be linear up to the value of load 12 KN in case of experiment.

The load and displacement values of experimental and analytical results are tabulated in Table 4.2

Table4.2 Comparison of Load and Displacement values of control RC slab

S. No.	Experimental results		Analytical results	
	Load (KN)	Displacement (mm)	Load (KN)	Displacement (mm)
1.	7	0.5	8.99	0.65
2.	14.53	3.70	15.50	1.20
3.	13.20	5	13.50	3.62
4.	16.09	11.60	15.80	9.41
5.	17.37	13.74	16.10	10.70
6.	19.12	15.20	17.30	11.70
7.	19.85	16.05	17.40	12.40
8.	20	16.70	14	14

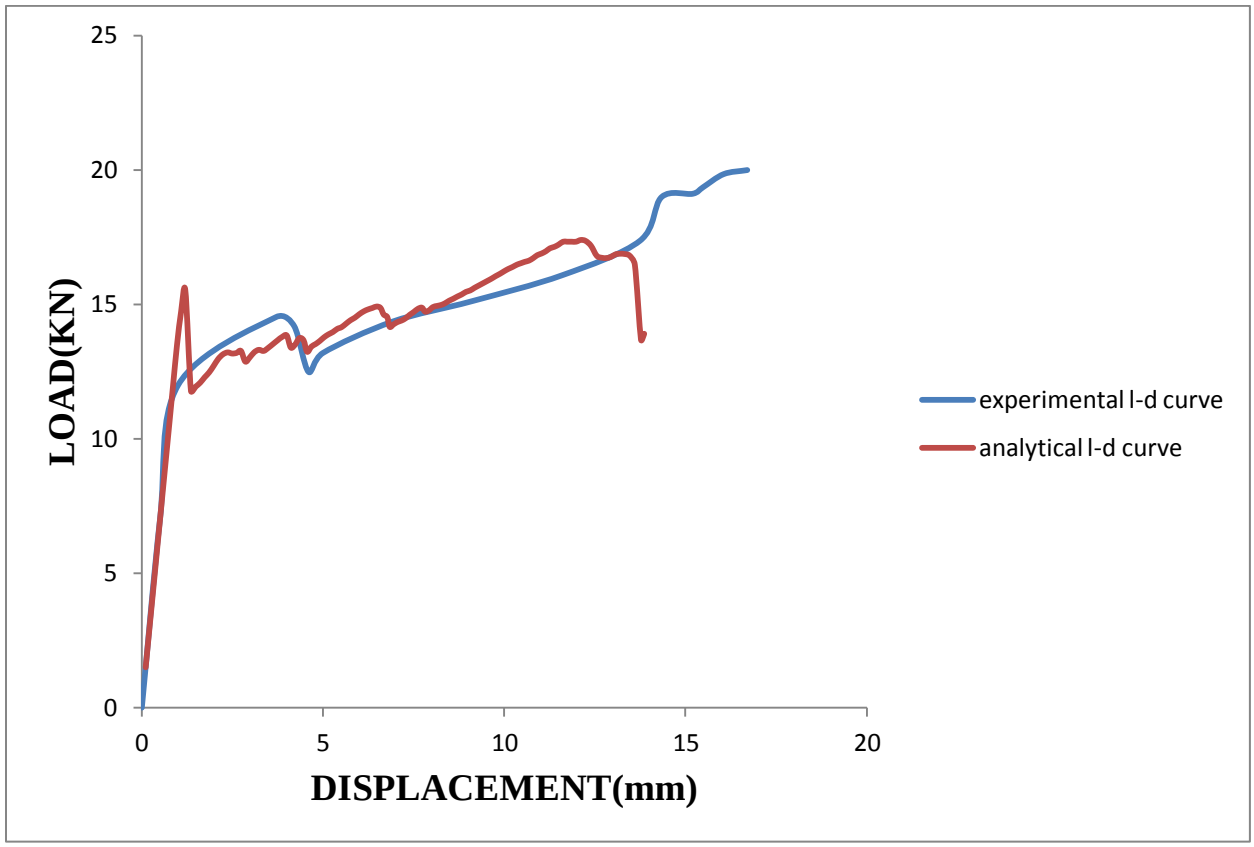

Figure 4.9 Comparison of Load-Displacement curve of control RC slab

4.4 FE MODEL RESULTS OF GFRP RETROFITTED RC SLAB

The non-linear response of retrofitted RC slab modelled as per details discussed in Chapter 3 using FE Modelling under the incremental loading has been carried out. The FRP modelling has been done as a 3D shell element in ATENA. The layer of GFRP has been applied at the bottom face of the slab. The effect of GFRP on the ultimate strength of slab, crack pattern and crack width has been discussed.

4.4.1 Load v/s Deformation of retrofitted RC slab

The area load on the structure has been applied in gradual increments up to its failure level. The behaviour of the slab at every step of load deflection is analyzed with the help of load-deflection curve, crack patterns and cracks propagation at every step. The load v/s deflection curve has been plotted in Figure 4.10. The retrofitted model has been found to behave linearly

elastic up to a value of 7.85 KN. Then with slight decrease in value of load, the value of load again increases from 7.40 KN to a value of 18.10 KN at 1.2 mm deflection. The curve depicted non-linearity as loss of stiffness has been observed, because of which the load value decreased 10.8 KN. After this point, as the load increased the value of deflection also increased. As the slab is strengthened with GFRP at the tension face, slab takes much higher load to a value of about 20.9 KN at a displacement value of 12.8 KN. The ultimate load carrying capacity of retrofitted slab has been observed as 20.90 KN.

The displacements at different values of load has been tabulated in Table 4.3

Table 4.3 The load and displacement values of the retrofitted slab

Load (KN)	Displacement (mm)
2.50	0.22
7.84	0.53
7.40	0.64
12.70	0.95
18.10	1.16
10.80	1.35
12.30	2.96
13.70	5.84
14.60	6.88
16.10	9.49
18.40	11.30
19.10	11.70
20.90	12.80

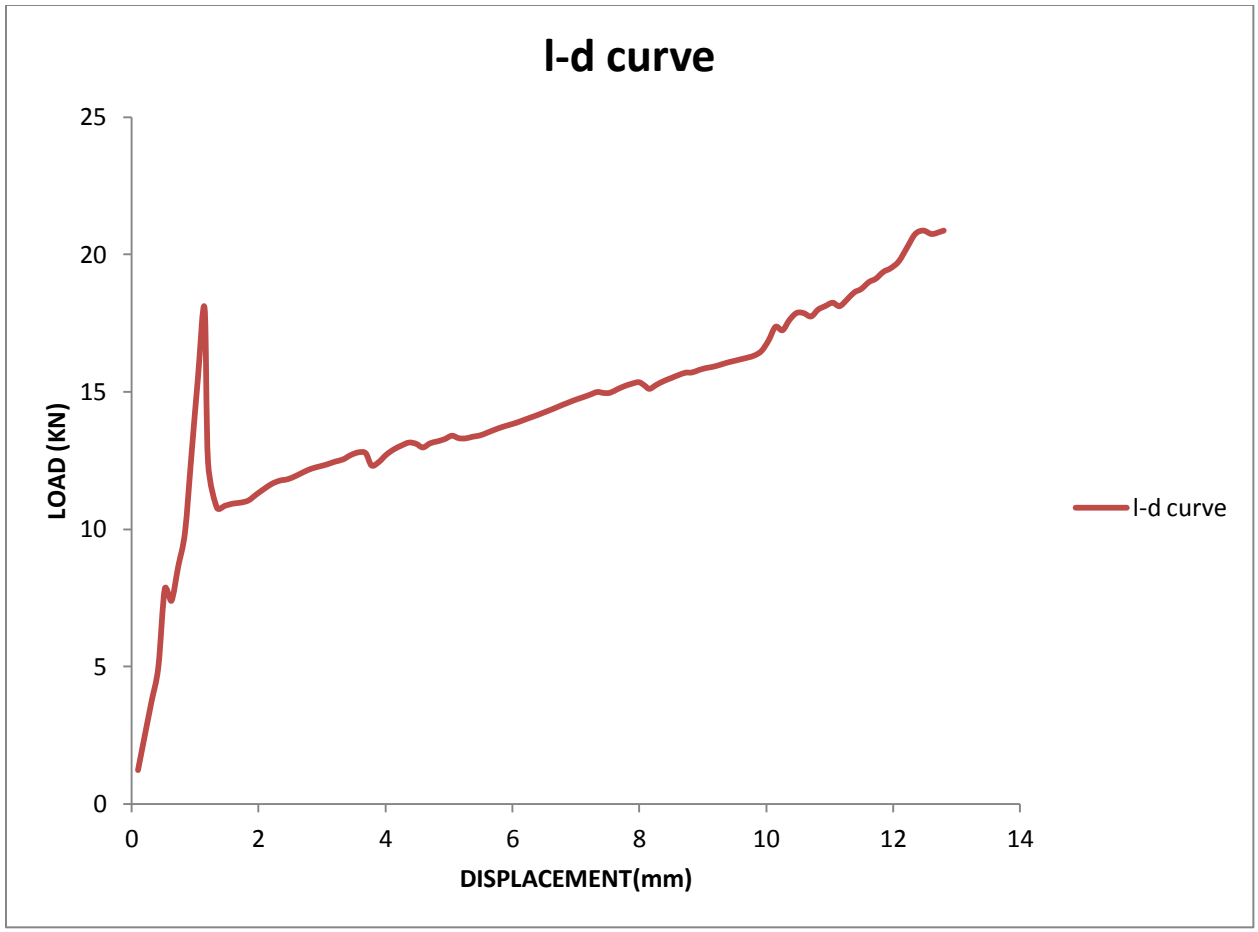

Figure 4.10 Load-Displacement curve of the retrofitted slab

4.4.2 Crack patterns

The variations of crack pattern due to applied load in slab are plotted in Figure 4.11-4.16 Discussions on crack patterns plotted below are presented. At the early stages of loading, the behaviour of the slab has been observed to be elastic until the appearance of the first crack. Invariably, the crack has been initiated at the centre of the slab and the cracks gradually propagate towards the ends on the tension face side as the loading progressed.

At load value of 7.84 KN it has been observed that micro-cracks appeared in the structure. The micro-cracks appeared when the slab is in linear zone. The cracks keep on increasing as the load and the deflection increases. Figure 4.11 shows that the first crack appeared in tension zone of slab which has been observed at load value of 18.1 KN at 1.16 mm deflection. The maximum crack width at this point is 0.1 mm.

Figure.4.11 Cracks of 0.1mm width at deflection of 1.16mm

After the peak load of 18.10 KN, the value of load decreases to 10.80 KN at deflection of 1.35 mm as shown in load- deflection curve above. The crack pattern is plotted in Figure 4.12**.** The cracks that appeared at the tension face of the slab became a bit wider and bigger. The maximum crack width at this point is 0.30 mm.

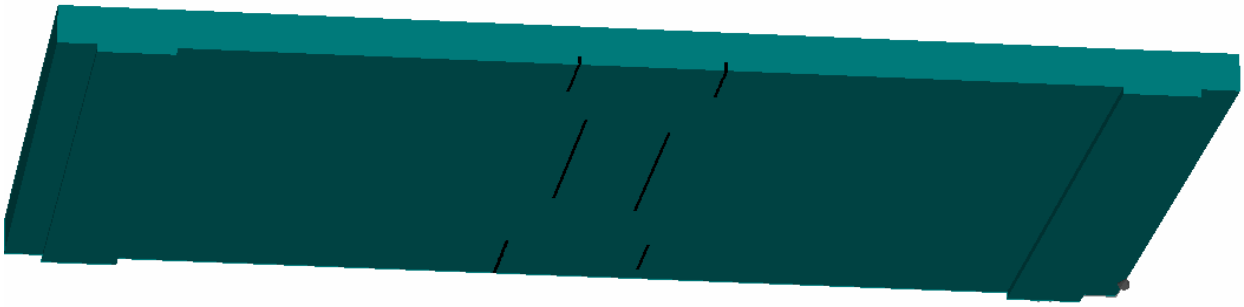

Figure 4.12 Cracks of 0.3mm width at deflection of 1.35mm

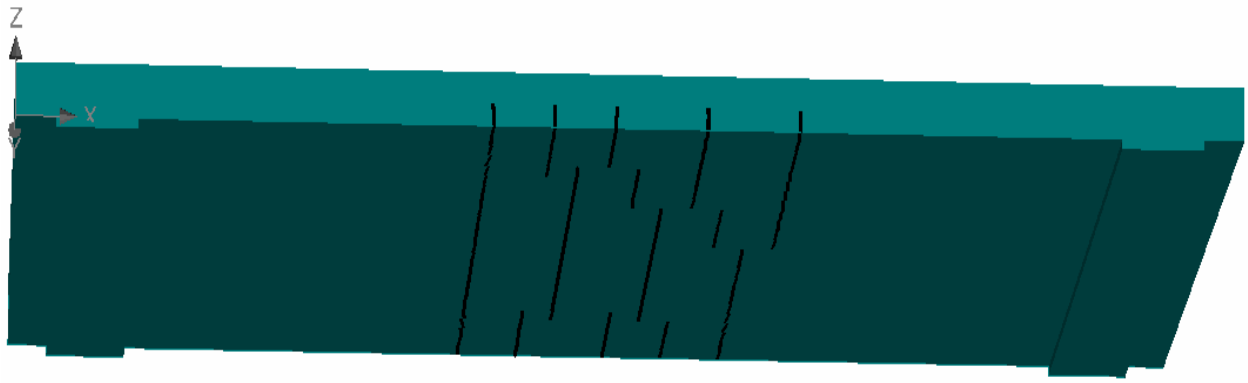

Figure 4.13 Cracks of 0.5mm width at deflection of 6.88mm

The cracks propagate in tension face from the centre which moves towards the free edge. The crack pattern corresponding to load value of 14.6 KN has been presented in Figure 4.13. The displacement of 6.88 mm has been observed at this stage. Flexure cracks which are observed in the tension zone of slab reduces the load carrying capacity of slab. Maximum width of crack at this load has been found to be 0.5 mm.

The crack pattern at maximum load at both top and bottom has been plotted in Figure 4.14 and Figure 4.15. It has been observed that the maximum load of 20.9 KN has been taken by the slab at a maximum deflection of 12.80 mm. The maximum width of crack at this stage is 1 mm and as plotted in Figure 4.16. Major damage has been noticed at the centre of the slab while there is no damage at the corner of the slab.

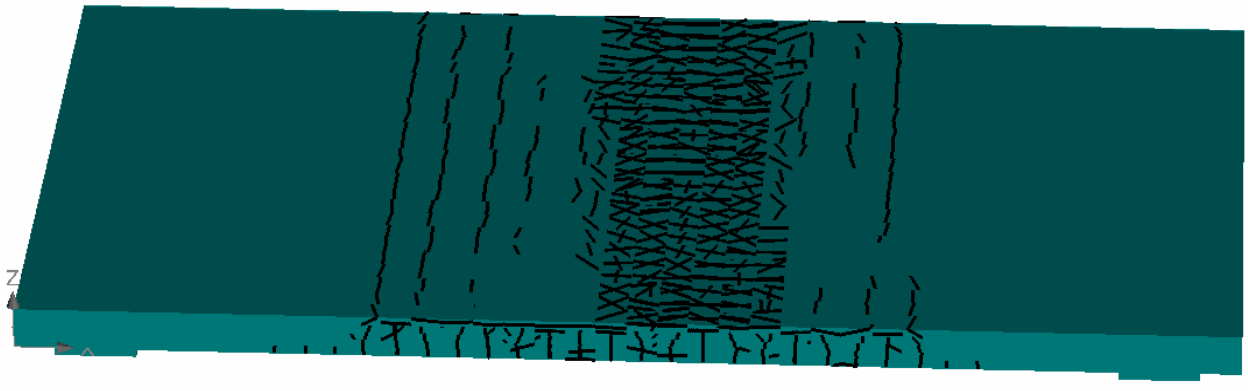

Figure.4.14 All cracks at top surface of the slab at deflection of 12.80mm

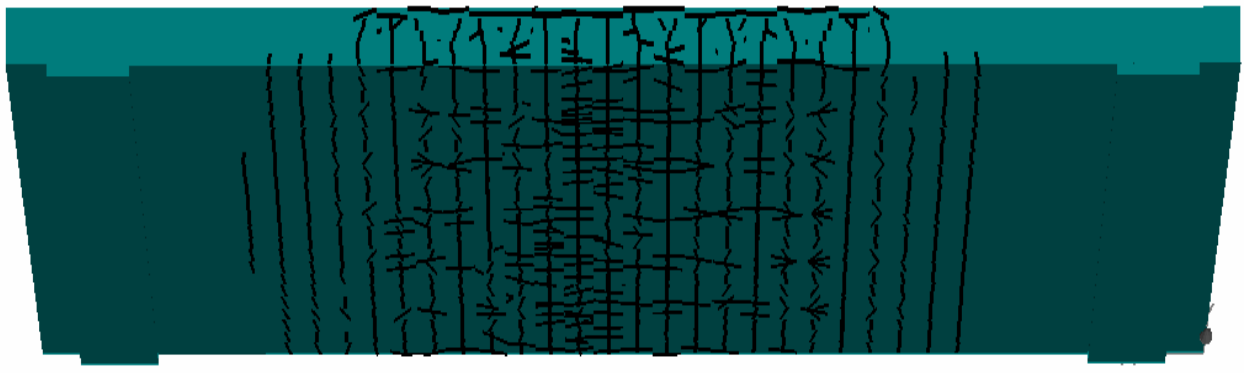

Figure 4.15 All cracks at bottom surface of the slab at deflection of 12.80mm

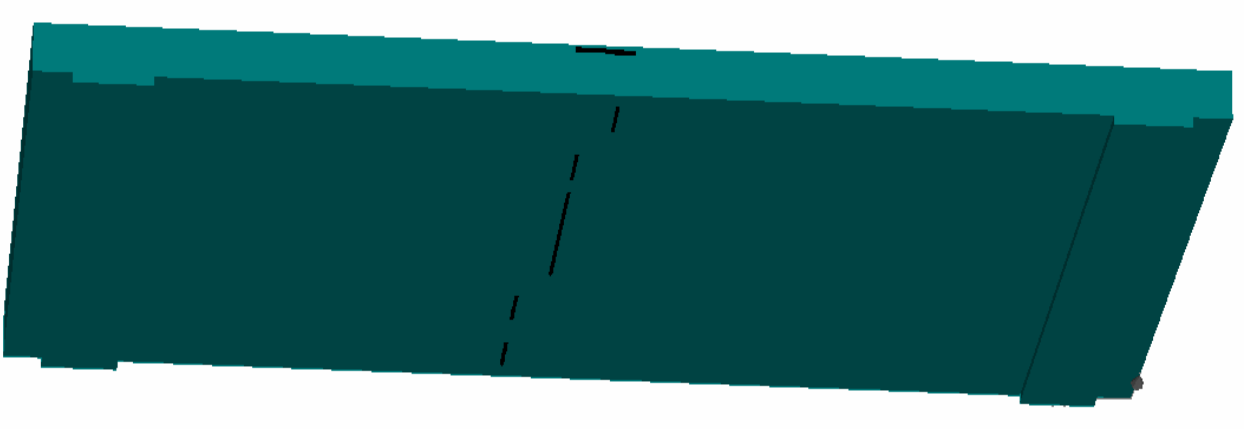

Figure 4.16 Cracks of 1mm width at deflection of 12.80mm

4.5 COMPARISON BETWEEN FE MODEL AND EXPERIMENTAL RESULTS OF THE RETROFITTED RC SLAB

4.5.1 Load v/s Deformation curve

The load-displacement curve plotted in Figure 4.17 shows the difference in the load carrying capacity of the slab. The result of analytical work has been compared with the experimental work done by Chothani.D.G. (2012). The ultimate load carrying capacity and maximum deflection of the slab according to experimental results was around 23.02 KN and 13.92mm respectively and the analytical load carrying capacity and maximum deflection has been observed as 20.90 KN and 12.80 mm respectively. The results of analytical work varied from experimental work as per the reasons mentioned above. The percentage increase in ultimate load carrying capacity of retrofitted slab as compared to the control slab has been observed as 20.2%.

The plot depicted that initially the analytical value of load has been observed higher than the experimental value. The behaviour of the slab has been observed to be almost linear up to the value of load around 18.10 KN in FE model with a slight bent whereas the structure has been found to be linear up to the value of load 9.87 KN in case of experiment. The analytical load value is higher from experimental till 14.5 KN, after this analytical load value is lesser than the experimental value whereas the deflection noticed in the FE model is 12.8 mm which is lesser than experimental value of 13.92 mm.

The load and displacement values of experimental and analytical results are tabulated in Table 4.4

Table4.4 Comparison of Load- Displacement values of retrofitted RC slab

S. No.	Experimental results		Analytical results	
	Load (KN)	Displacement (mm)	Load (KN)	Displacement (mm)
1.	6.20	0.4	7.84	0.53
2.	7.10	0.7	7.40	0.64
3.	9.87	1.12	18.10	1.16
4.	10.81	4.96	10.80	1.35
5.	16.09	7.40	12.80	3.70
6.	19.86	10	14.60	6.88
7.	22.04	12.30	17.30	10.30
8.	23.02	13.92	20.90	12.80

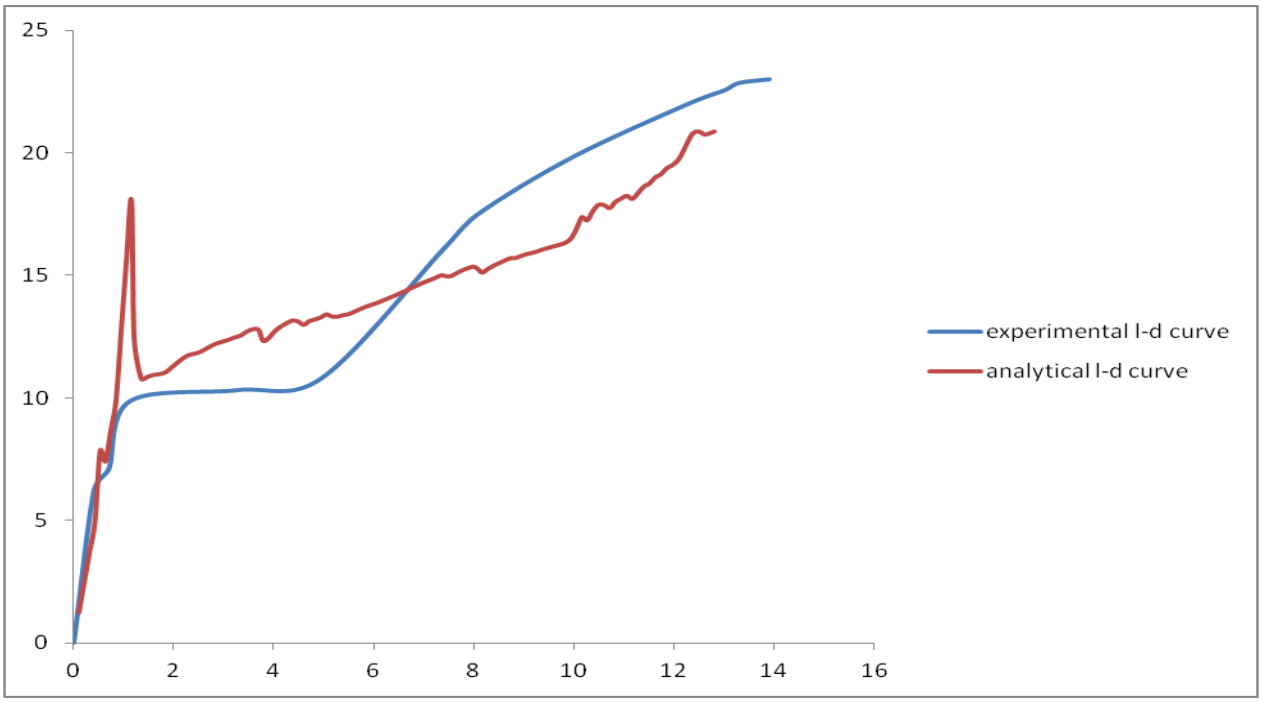

Figure 4.17 Comparison of Load-Displacement curve of retrofitted RC slab

4.6 FE MODEL RESULTS OF 75% STRESSED RETROFITTED RC SLAB

In the present study, non-linear response of stressed retrofitted RC slab is modelled as per details discussed in Chapter 3 using FE Modelling under the incremental area load has been carried out. The FE model of the slab is first stressed to 75% and then the slab has been strengthened using GFRP sheets. The variation of load- displacement graph, the crack patterns, propagation of the cracks and the crack width at different values of load has been studied.

4.6.1 Load v/s Deformation of 75% stressed retrofitted RC slab

The load has been applied as area load on the top surface of the slab in gradual increments up to failure load. The behaviour of the slab at every step of load deflection is analyzed with the help of load-deflection curve, crack patterns and cracks propagation at every step. The load v/s deflection curve has been plotted in Figure 4.18.

The 75% stressed retrofitted model has been found to behave almost linearly elastic up to a load value of 14.30 KN. Then with decrease in value of load, the value of load again increases from 11.70 KN to a value of 14.30 KN at 1.61 mm deflection. The curve depicted non-linearity as loss of stiffness has been observed, because of which the load value again decreased to 10.9 KN. After this point, as the load increased the value of deflection also increased. As the slab is strengthened with GFRP at the tension face, slab takes much higher load to a value of about 19 KN at a displacement value of 13.5 KN. The ultimate load carrying capacity of 75% stressed retrofitted slab has been observed as 19 KN.

The displacements at different values of load has been tabulated in Table 4.5

Table 4.5 The load and displacement values of 75% stressed retrofitted slab

Load (KN)	Displacement (mm)
3.02	0.33
7.55	0.82
14.30	1.13
11.70	1.27
14.30	1.61

10.90	2.02
12.50	3.34
13.80	4.48
15.30	7.23
16.80	8.81
17.40	9.95
19	13.50
14.70	14.40

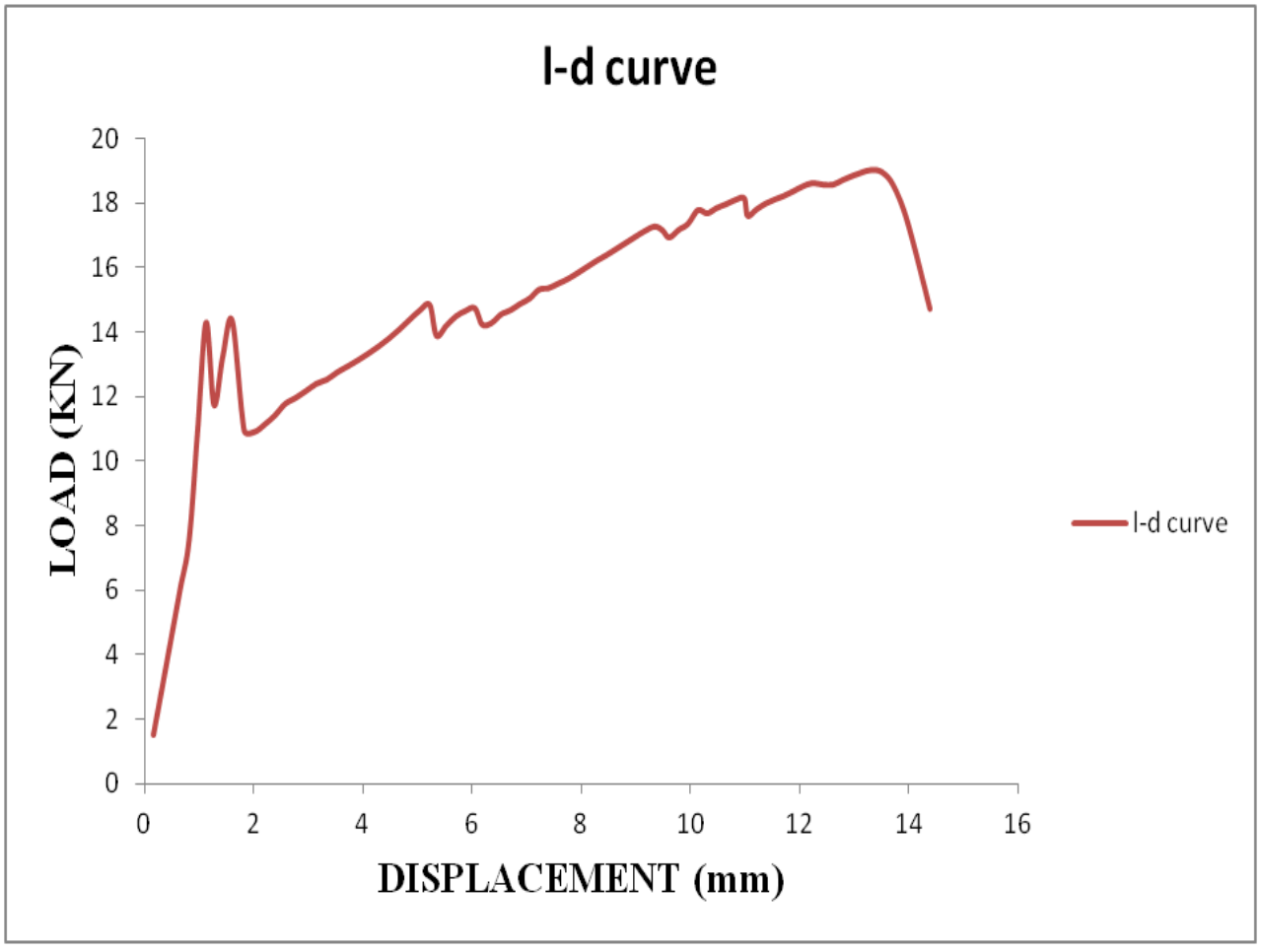

Figure 4.18 Load-Displacement curve of 75% stressed retrofitted slab

4.6.2 Crack patterns

The variations of crack pattern due to applied load in slab are plotted in Figure 4.19-4.27 Discussions on crack patterns plotted below are presented. At the early stages of loading, the behaviour of the slab has been observed to be elastic until the appearance of the first crack. Invariably, the crack was initiated at the centre of the slab and the cracks gradually propagate towards the ends on the tension face side as the loading progressed.

At load value of 14.30 KN it has been observed that micro-cracks appeared in the structure. The micro-cracks appeared when the slab is in linear zone. The load decreases to a value of 11.70 KN and the micro-cracks increases as the load and the deflection increases. Figure 4.19 shows that the first crack appeared in tension zone of slab which has been observed at load value of 11.7 KN at 1.27 mm deflection. The maximum crack width at this point is 0.15 mm.

Figure 4.19 Cracks of 0.15mm width at deflection of 1.27mm

The cracks propagate towards the free edge of the slab. After the load value of 11.70 KN the slab again gains stiffness and reaches a value of 14.30 KN at deflection of 1.61 mm. The crack pattern at load 14.30 KN is plotted in Figure 4.20. The maximum crack width is 0.31 mm. Further again the load value decreases to 10.9 KN and the value of deflection has been observed as 2.02 mm as shown in load- deflection curve above. The crack pattern is plotted in Figure 4.21. The cracks that appeared at the tension face of the slab became a bit wider and bigger. The maximum crack width at this point is 0.37 mm. This decrease in load is because of the widening of cracks in the slab.

Figure 4.20 Cracks of 0.31mm width at deflection of 1.61mm

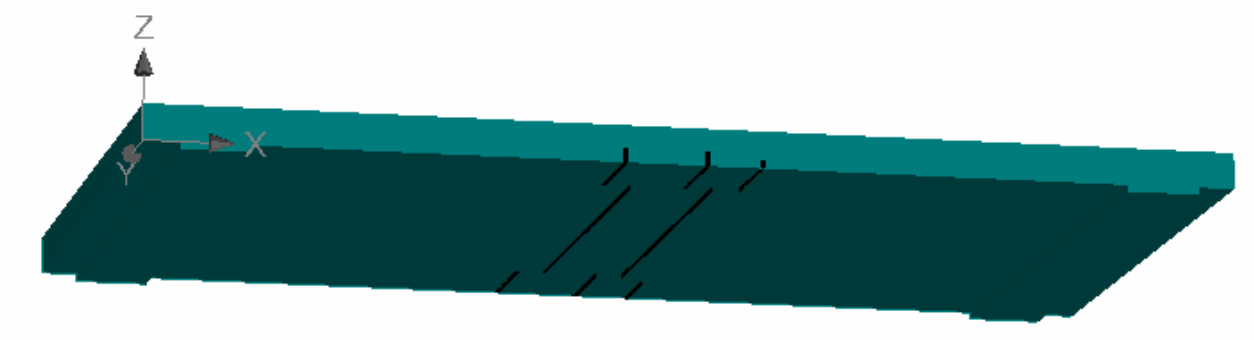

Figure 4.21 Cracks of 0.37 mm width at deflection of 2.02mm

The crack patterns at load value of 16.80 KN are presented in Figure 4.22. The displacement of 8.81 mm has been observed corresponding to load value of 16.80 KN. Flexure cracks which are observed in the tension zone of slab reduces the load carrying capacity of slab. Maximum width of crack at this load has been found to be 0.68 mm.

Figure 4.22 Cracks of 0.68mm width at deflection of 8.81mm

The maximum load taken by the slab has been observed as 19 KN at a deflection of 13.5 mm and the crack pattern at this stage has been plotted in Figure 4.23. The maximum size of crack at maximum load value is 1.20 mm. The crack pattern at both top and bottom has been plotted in Figure 4.24 and Figure 4.25. Major damage has been noticed at the centre of the slab while there is no damage at the corner of the slab.

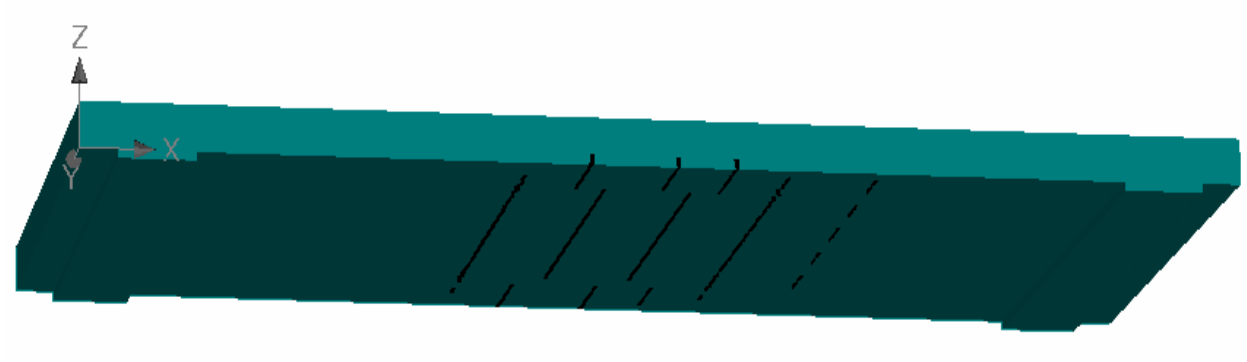

Figure 4.23 Cracks of 1.20mm width at deflection of 13.5mm

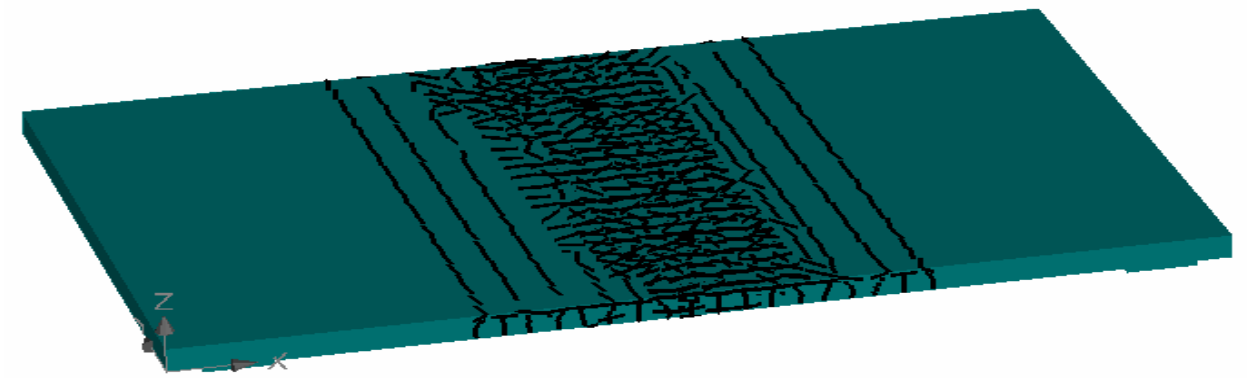

Figure 4.24 All cracks at top surface of the slab at deflection of 13.5mm

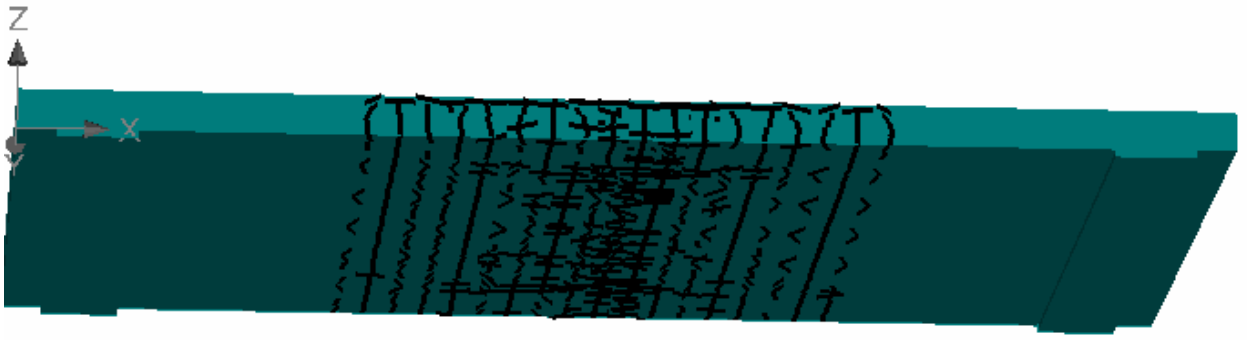

Figure 4.25 All cracks at bottom surface of the slab at deflection of 13.5mm

4.7 COMPARISON BETWEEN THE ANALYTICAL RESULTS OF CONTROL SLAB AND 75% STRESSED RETROFITTED SLAB

The comparison of load-displacement curve for control slab and 75% stressed retrofitted slab has been plotted below in Figure 4.26.

In the control slab and 75% stressed retrofitted slab, the behaviour of slab has been observed to be linear up to a load value of 15.5 KN and 14.30 KN respectively. At this point, flexural cracks started appearing at the bottom of the slab and then load value decreases. The slab gains stiffness and load starts increasing with increase in deflection. The load in 75% stressed retrofitted slab increase more because of the GFRP sheet. The GFRP sheet increases the load carrying capacity of the slab. The cracks propagate at the centre and moves towards the free edge of the slab. The ultimate load taken by the retrofitted slab has been observed as 19 KN and that of the control slab is 17.4 KN. The stiffness of the slab further decreases and load carrying capacity decreases. The maximum width of the crack has been observed as 1 mm in control slab and in 75% stressed retrofitted slab has been observed as 1.20 mm. Flexural failure of the slab is the prominent mode of failure and severe damage has been observed at the centre of the slab. The percentage increase in load carrying capacity of 75% stressed retrofitted slab as compared to control slab has been observed as 10.5%.

The load and displacement values of control and 75% stressed retrofitted slab results are tabulated in Table 4.6

Table 4.6 Comparison of Load- Displacement values of control and 75% stressed retrofitted slab

S. No.	Control slab		75% stressed retrofitted slab	
	Load (KN)	Displacement (mm)	Load (KN)	Displacement (mm)
1.	8.99	0.65	7.55	0.82
2.	15.50	1.20	14.30	1.13
3.	13.50	3.62	11.7	1.27
4.	15.80	9.41	14.30	1.61
5.	16.10	10.70	10.90	2.02
6.	17.30	11.70	16.80	8.81

7.	17.40	12.40	19	13.50
8.	14	14	14.70	14.40

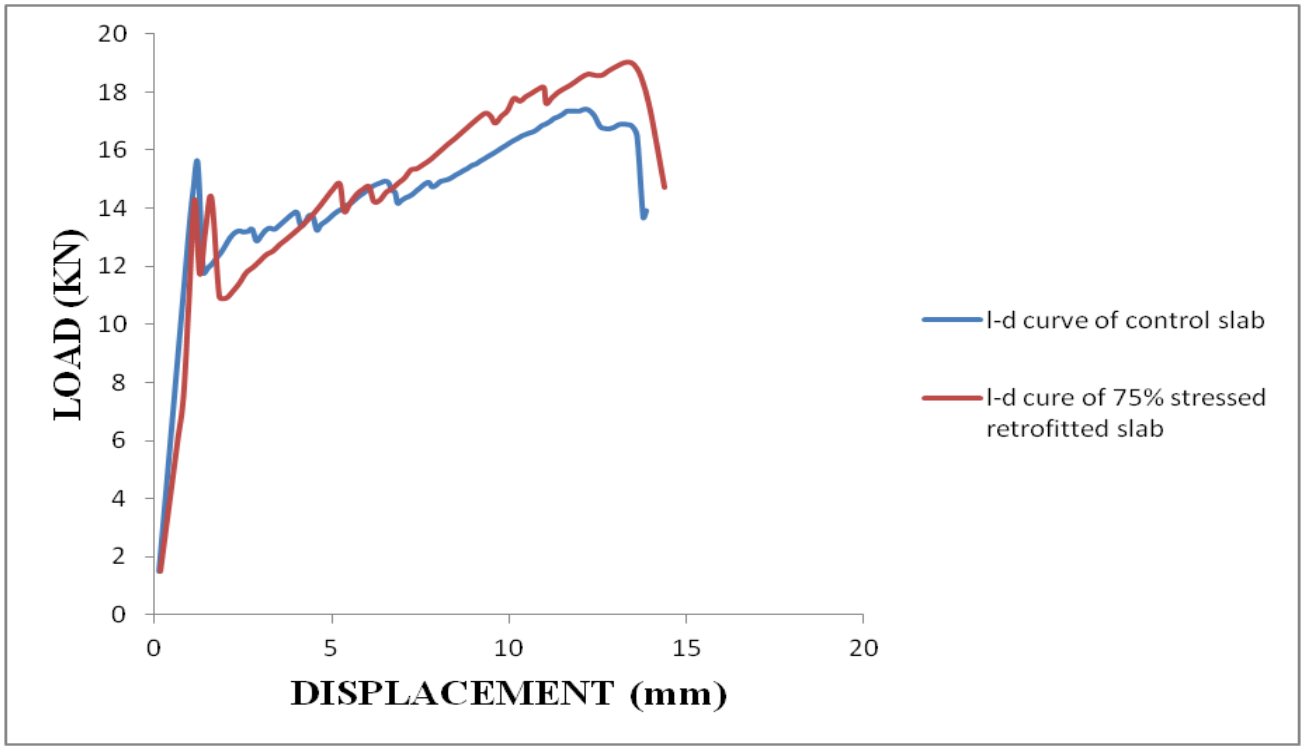

Figure 4.26 Comparison of Load-Displacement curves of control and 75% stressed retrofitted slab

4.8 FE MODEL RESULTS OF 90% STRESSED RETROFITTED RC SLAB

The FE model of the slab is first stressed to 90% and then the slab has been strengthened using GFRP sheets. The variation of load- displacement graph, the crack patterns, propagation of the cracks and the crack width at different values of load has been studied.

4.8.1 Load v/s Deformation of 90% stressed retrofitted RC slab

The load has been applied as area load on the top surface of the slab in gradual increments up to failure load. The behaviour of the slab at every step of load deflection is analyzed with the

help of load-deflection curve, crack patterns and cracks propagation at every step. The load v/s deflection curve has been plotted in Figure 4.27.

The 90% stressed retrofitted model has been found to behave almost linearly elastic up to a load value of 13.10 KN. Then with decrease in value of load, the value of load again increases from 10.90 KN to a value of 13.30 KN at 4.16 mm deflection. The curve depicted non-linearity as loss of stiffness has been observed, because of which the load value again decreased to 12.10 KN at deflection of 4.58 mm. After this point, as the load increased the value of deflection also increased. As the slab has been strengthened with GFRP at the tension face, slab takes much higher load to a value of about 18.40 KN at a displacement value of 13.2 KN. The ultimate load carrying capacity of 90% stressed retrofitted slab has been observed as 18.40 KN.

The displacements at different values of load has been tabulated in Table 4.5

Table 4.7 The load and displacement values of 90% stressed retrofitted slab

Load (KN)	Displacement (mm)
3	0.42
6.39	0.62
9.24	1.03
13.10	1.84
10.90	2.41
13.30	4.16
12.10	4.58
14.50	6.89
15.70	8.06
16.60	10.60
17.20	11.50

18.40	13.20
15	14.3

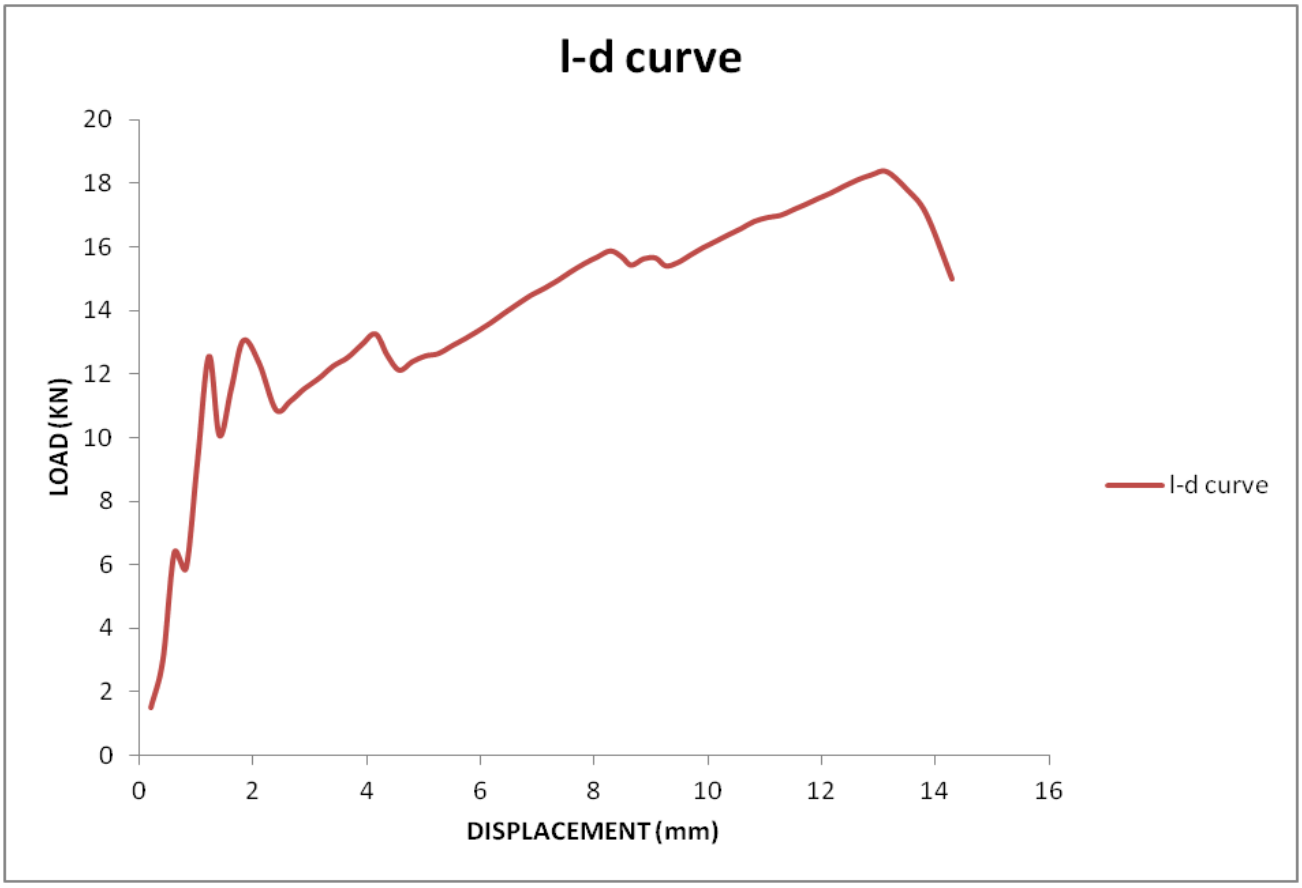

Figure 4.27 Load-Displacement curve of 90% stressed retrofitted slab

4.8.2 Crack patterns

The variations of crack pattern due to applied load in slab are plotted in Figure 4.28-4.37 Discussions on crack patterns plotted below are presented. At the early stages of loading, the behaviour of slab has been observed to be elastic until the appearance of the first crack whereas the micro-cracks appeared in the linear zone only. Invariably, the crack has been initiated at the centre of the slab and the cracks gradually propagate towards the ends on the tension face side as the loading progressed.

At load value of 13.10 KN it has been observed that micro-cracks appeared in the structure. The micro-cracks appeared when the slab is in linear zone. The load decreases to a value of 10.90 KN and the micro-cracks increases as the load and the deflection increases. Figure 4.28 shows that the first crack appeared in tension zone of slab which has been observed at load value of 10.90 KN at 2.41 mm deflection. The maximum crack width at this point is 0.12 mm.

Figure 4.28 Cracks of 0.12mm width at deflection of 2.41mm

The cracks propagate towards the free edge of the slab. After the load value of 10.90 KN the slab again gains stiffness and reaches a value of 13.30 KN at deflection of 4.16 mm. The crack pattern at load 13.30 KN is plotted in Figure 4.29. The maximum crack width is 0.46 mm. Further again the load value decreases to 12.10 KN and the value of deflection has been observed as 4.58 mm as shown in load- deflection curve above. The crack pattern is plotted in Figure 4.30. The cracks that appeared at the tension face of the slab became a bit wider and bigger. The maximum crack width at this point is 0.49 mm. This decrease in load is because of the widening of cracks in the slab.

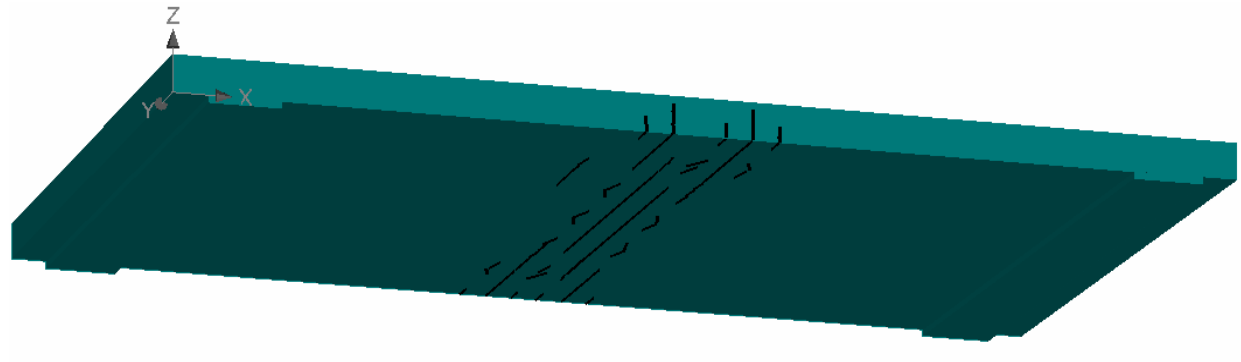

Figure 4.29 Cracks of 0.46mm width at deflection of 4.16mm

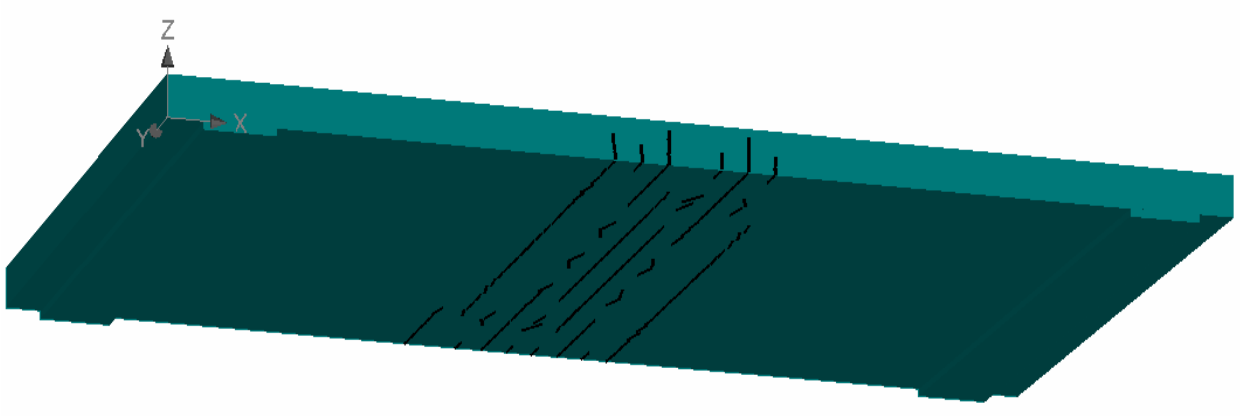

Figure 4.30 Cracks of 0.49mm width at deflection of 4.58mm

The crack patterns at load value of 15.70 KN are presented in Figure 4.31 and the displacement of 9.69 mm has been observed at this stage. Flexure cracks which are observed in the tension zone of slab reduce the load carrying capacity of slab. Maximum width of crack at this load has been found to be 0.62 mm. The cracks and the deflection keep on increasing as the value of load increases.

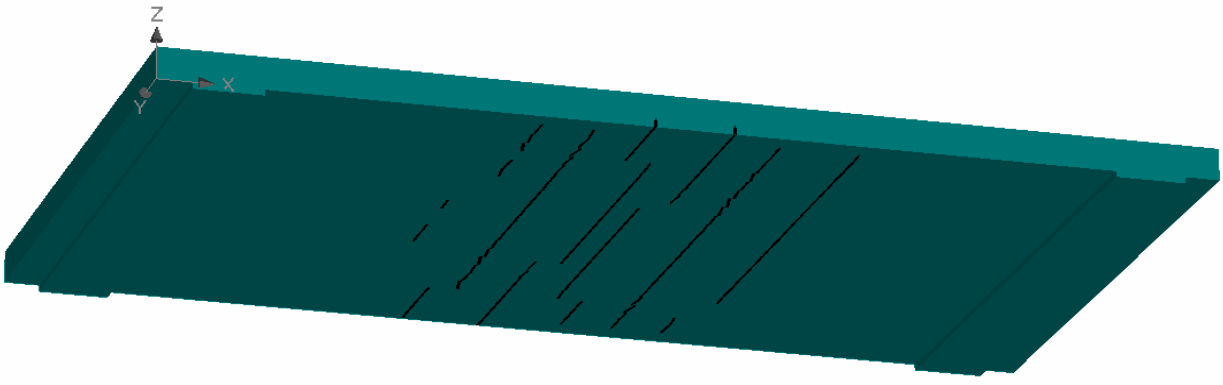

Figure4.31 Cracks of 0.62mm width at deflection of 9.69mm

The maximum load taken by the slab has been observed as 18.40 KN at a deflection of 13.20 mm. The crack pattern at maximum load has been plotted in Figure 4.32. The maximum width of crack at maximum load value is 1.18 mm. The crack pattern at both top and bottom has been plotted in Figure 4.33 and Figure 4.34. Major damage has been noticed at the centre of the slab while there is no damage at the corner of the slab.

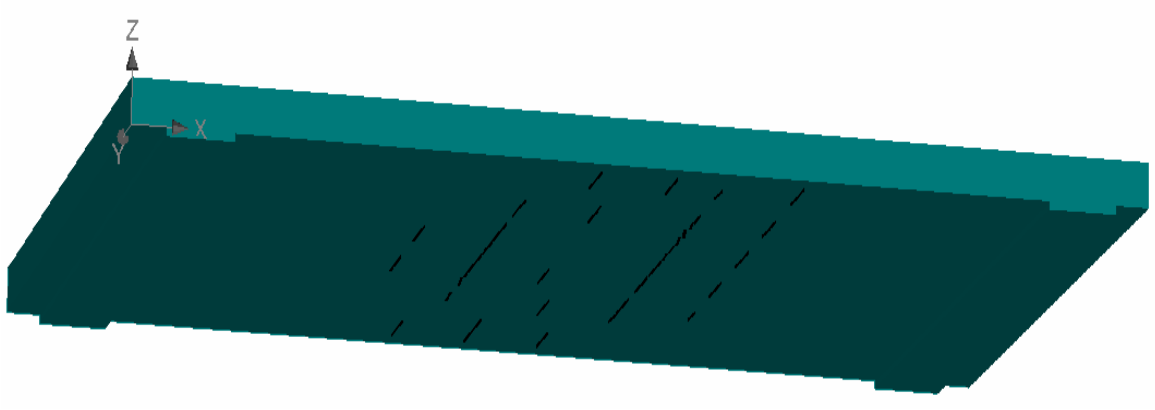

Figure 4.32 Cracks of 1.18mm width at deflection of 13.2mm

Figure 4.33 All cracks at top surface of the slab at deflection of 13.2mm

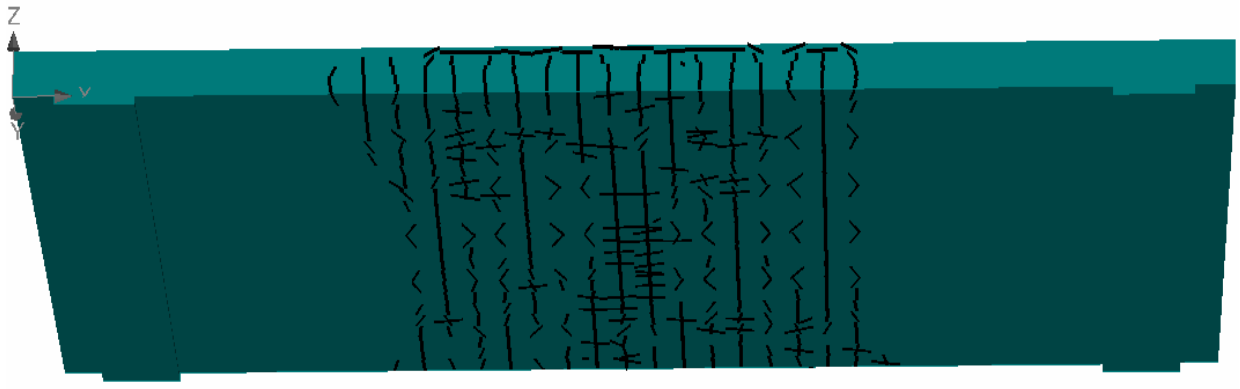

Figure 4.34 All cracks at bottom surface of the slab at deflection of 13.2mm

4.9 COMPARISON BETWEEN THE ANALYTICAL RESULTS OF CONTROL SLAB AND 90% STRESSED RETROFITTED SLAB

The comparison of load-displacement curve for control slab and 90% stressed retrofitted slab has been plotted below in Figure 4.35.

In the control slab and 90% stressed retrofitted slab, the behaviour of slab has been observed to be linear up to a load value of 15.5 KN and 13.10 KN respectively. At this point, flexural cracks started appearing at the bottom of the slab depicting reduction in stiffness and the load value also decreases. The slab gains stiffness and load starts increasing with increase in deflection. The load in 90% stressed retrofitted slab increase more because of the GFRP sheet. The GFRP sheet increases the load carrying capacity of the slab. The cracks propagate at the centre and moves towards the free edge of the slab. The ultimate load taken by the retrofitted slab has been observed as 18.4 KN and that of the control slab is 17.4 KN. The stiffness of the slab further decreases and load carrying capacity decreases. The maximum width of the crack has been observed as 1 mm in control slab and in 90% stressed retrofitted slab has been observed as 1.18 mm. Flexural failure of the slab is the prominent mode of failure and severe damage has been observed at the centre of the slab. the percentage increase in ultimate load carrying capacity of 90% stressed retrofitted slab as compared to the control slab has been observed as around 6%

The load and displacement values of control and 90% stressed retrofitted slab results are tabulated in Table 4.8

Table 4.8 Comparison of Load- Displacement values of control and 90% stressed retrofitted slab

S. No.	Control slab		90% stressed retrofitted slab	
	Load (KN)	Displacement (mm)	Load (KN)	Displacement (mm)
1.	8.99	0.65	6.39	0.63
2.	15.50	1.20	13.10	1.84
3.	13.50	3.62	10.90	2.41
4.	15.80	9.41	13.30	4.16

5.	16.10	10.70	12.1	4.58
6.	17.30	11.70	15.70	9.69
7.	17.40	12.40	18.40	13.20
8.	14	14	15	14.30

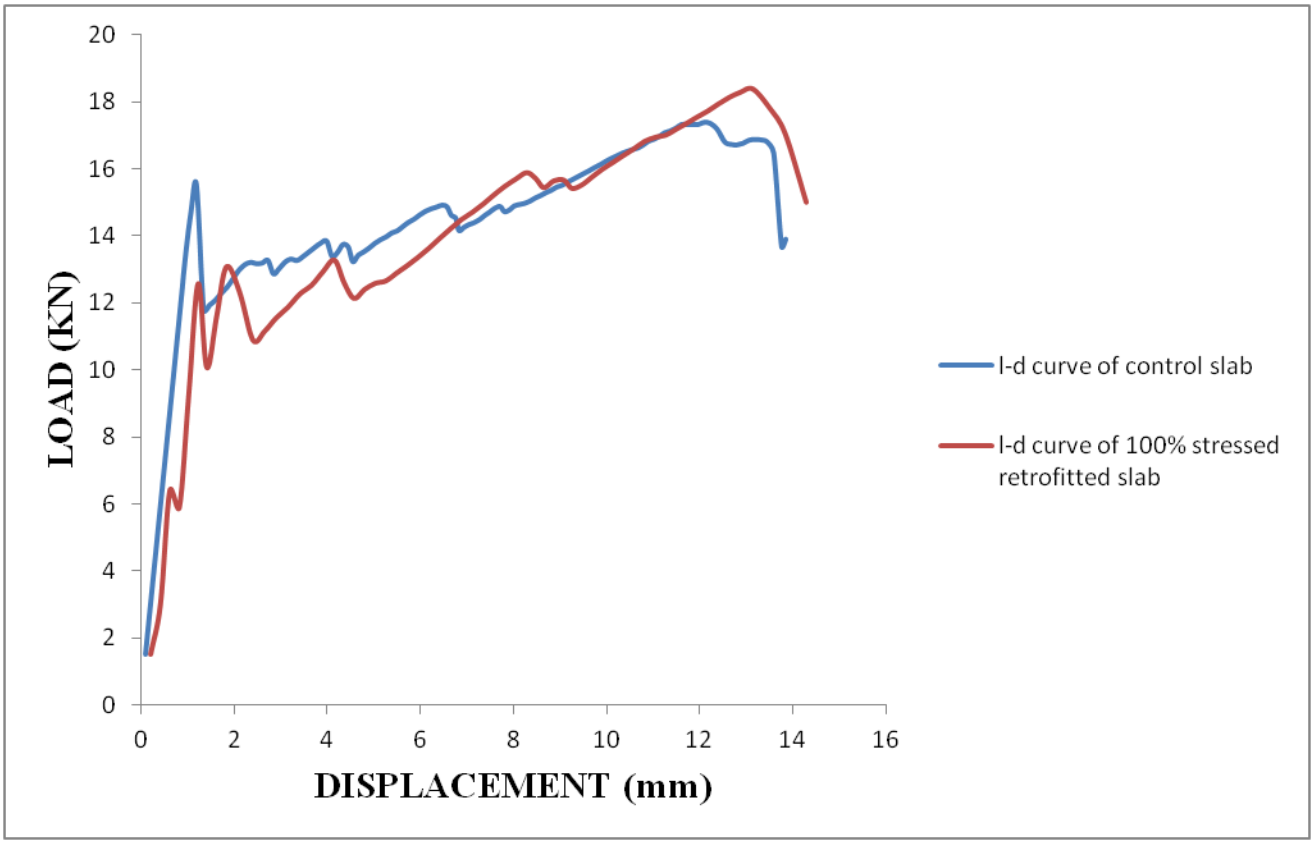

Figure 4.35 Comparison of Load-Displacement curves of control and 90% stressed retrofitted slab

CHAPTER 5 CONCLUSIONS AND RECOMMENDATIONS

5.1 GENERAL

In the present study, the non-linear response of RC control slab, the retrofitted RC slab and the stressed retrofitted slab at 75% and 90% using FE Modelling under the incremental area loading has been carried out with the intention to study the relative importance of several factors in the non-linear finite element analysis of RC slab.

5.2 CONCLUSIONS

The main observations and conclusions drawn from the study are listed below:

- The behaviour of slab represented by the load-deflection curves in ATENA show close agreement with the experimental data from the full-scale RC slab tests.
- It has been concluded that retrofitting the slab with GFRP, the cracks appear lesser and the crack width also reduces and the slab also bears larger deflection and retrofitting the slab with GFRP sheet also increases the ultimate load carrying capacity of the slab.
- The analytical load carrying capacity of the control slab was in close agreement with the experimental work.
- In the analytical results, the load carrying capacity of retrofitted slab has increased by 20% as compared to the control slab.
- Analytically the load carrying capacity of the 75% stressed and 90% stressed retrofitted slab has increased to 10.5% and 6% respectively as compared to the control slab.
- The higher value of ultimate load for the retrofitted specimen is associated with lower deflections as compared to the control specimen in the analysis performed in ATENA.
- The cracks start appearing at the centre and move from centre towards the free edges of the slab. Major damage occurred at the centre of the slab and negligible damage occurred at corners.

5.3 FUTURE SCOPE

In the present study one-way slab has been studied under monotonic incremental loading. The behaviour of two-way slab can also be studied in future. An investigation on the effect of

different span/depth and aspect ratios on the structural behaviour of the one-way FRP slab can also be studied. Retrofitted slab at various stress levels and with different types of FRP wrapping can be studied to observe their behaviour at different loadings.

REFERENCES

1. Mehta, A. (2011), **"Effect of initial stress levels on strength of beams retrofitted using pre-stressed fibre composites"** M.E. Thesis, Thapar University, Patiala.

2. Cervenka, V., Cervenka, J., & Pukl, R. **"ATENA—A tool for engineering analysis of fracture in concrete."** Sadhana 27.4 (2002): 485-492.

3. Chothani, D.G., Arora, N.K., and Dave, S.P."**Effect of anchoring GFRP sheet on ultimate strength of slab."** Fourth International Conference on Structural Stability and Dynamics (ICSSD 2012), 4–6 January, 2012.

4. Kenneth, W. N., Ahmed, G., Hussien, M. A. B., Walid, E. E., and Usama, A. E. **"Approaches for finite element simulations of FRP-strengthened concrete beams and slabs."** Architecture, 4.4 (2011): 59-72.

5. Kim, Y. J., Longworth, J. M., Wight, R. G., & Green, M. F. **"Flexure of two-way slabs strengthened with prestressed or nonprestressed CFRP sheets."** Journal of Composites for Construction, 12.4 (2008): 366-374.

6. Maaddawy, T. El., and Soudki. K. **"Strengthening of reinforced concrete slabs with mechanically-anchored unbonded FRP system."** Construction and Building Materials 22.4 (2008): 444-455.

7. Elsayed, W., Usama A. E., and Kenneth W. N. **"Interfacial behavior and debonding failures in FRP-strengthened concrete slabs."** Journal of Composites for Construction 11.6 (2007): 619-628.

8. Limam, O., Viet Tung, N., and Foret, G. **"Numerical and experimental analysis of two-way slabs strengthened with CFRP strips."**Engineering structures 27.6 (2005): 841-845.

9. Limam, O., Foret, G. and Ehrlacher. A. **"RC two-way slabs strengthened with CFRP strips: experimental study and a limit analysis approach."** Composite structures 60.4 (2003): 467-471.

10. Mosallam, A. S., and Mosalam, K. M. **"Strengthening of two-way concrete slabs with FRP composite laminates."** Construction and building materials 17.1 (2003): 43-54.

11. Lam, L., and Teng J. G. **"Strength of RC cantilever slabs bonded with GFRP strips."** Journal of Composites for Construction 5.4 (2001): 221-227.

12. Teng, J. G., Cao, S. Y., and Lam. L. **"Behaviour of GFRP-strengthened RC cantilever slabs."** Construction and Building Materials 15.7 (2001): 339-349.

13. IS 13920-1993 Edition 1.2 (2002-03), **"Indian Standard Code of Practice Ductile Detailing of Reinforced Concrete Structures Subjected to Seismic Forces"**, Bureau of Indian Standards, New Delhi, 2002.

14. IS 456: 2000 (Fourth Revision**), "Indian Standard: Plain and Reinforced Concrete – Code of Practice"**, Bureau of Indian Standards, New Delhi, 2005.

15. Kwak, H.G., Fillipou, C.F. **"Finite Element Analysis of Reinforced Concrete Structures Under Monotonic Loading"** Structural Engineering Mechanics and Materials**,** (1990) Report no. UCB/ SEMM-90/14.

16. A report on (2010) **" Strengthening of bridges using composite fibre wrapping technology for introduction of higher axle loads on indian railways "** compiled by D.Anjaneyulu Reddy and T.Muralidhara Rao.

17. Singhal, H. (2009), **"Finite Element Modeling of Retrofitted RCC Beams"** M.E. Thesis, Thapar University, Patiala.

18. Sharma, M. (2011), **"Finite Element Modelling of Reinforced Cement Concrete Skew Slab"** M.E. Thesis, Thapar University, Patiala.

19. ATENA 3D and ATENA WIN **–"Finite element software manuals".**

20. ATENA theory manual, part 1 from **Vladimir Cervenka, Libor Jendele and Jan Cervenka**.

21. A report on **"Use of FRP in strengthening/rehabilitation of concrete structures"** compiled by Rama Kant Gupta.

22. Rai, G., & Indolia, Y. (2011) **“Fiber Reinforced Polymer Composites, A novel way for strengthening structures”.**

23. GangaRao, H. V., Taly, N., & Vijay, P. V. **“Reinforced concrete design with FRP composites”** (2006) CRC press